DEVELOPMENT OF A NON-SOLVENT BASED TEST METHOD FOR

EVALUATING RECLAIMED ASPHALT PAVEMENT MIXES

Except where reference is made to the work of others, the work described in this dissertation is my own or was done in collaboration with my advisory committee. This dissertation does not include proprietary or classified information

_____

Alan Carter

Certificate of Approval:

_____   _____

Dr. Dan Brown   Dr. Mary Stroup-Gardiner, Chair
Associate Professor   Associate Professor
Civil Engineering   Civil Engineering

_____   _____

Dr. David Timm   Dr. Stephen L. McFarland
Assistant Professor   Acting Dean
Civil Engineering   Graduate School

DEVELOPMENT OF A NON-SOLVENT BASED TEST METHOD FOR

EVALUATING RECLAIMED ASPHALT PAVEMENT MIXES

Alan Carter

A Dissertation

Submitted to

The Graduate Faculty of

Auburn University

In Partial Fulfillment of the

Requirements for the Degree of

Doctor of Philosophy

Auburn, Alabama

August 8, 2004

DISSERTATION ABSTRACT

DEVELOPMENT OF A NON-SOLVENT BASED TEST METHOD FOR

EVALUATING RECLAIMED ASPHALT PAVEMENT MIXES

Alan Carter
Doctor of Philosophy, August 8, 2005
(M. Eng., Ecole de technologie supérieure, 2002)
(B.Eng., Ecole de technologie supérieure, 2000)

118 Typed Pages

Directed by Mary Stroup-Gardiner

The objectives of this research are twofold. The first is to develop and validate an indirect tension stress relaxation test methodology for assessing asphalt binder properties using compacted hot mix asphalt (HMA) samples. The second is to evaluate the influence of adding various percentages of reclaimed asphalt material (RAP) to HMA mixtures using this stress relaxation test. More than 32 different HMA mixtures (two binders, two aggregate sources, two sources of reclaimed asphalt pavement (RAP) used at five different percentages, three replicates) were compacted and tested using indirect tension stress relaxation test at two temperatures (5 and 22°C).

Two relaxation characteristics were used to evaluate binder properties in the compacted HMA samples: 1) the initial stress relaxation modulus (at time=1 second), and 2) the curvature coefficient (exponent) from a power law model fit to the data for each mix.

The stress relaxation test showed that the addition of RAP increases the modulus linearly from 0 to 50% of RAP but that there is no statistically significant change in modulus when increasing the percent RAP above 50%. The curvature coefficient decreases linearly with the increase of the percent RAP from 0 to 50%, but like for the modulus, there is no statistically significant change in curvature coefficient when increasing the percent RAP above 50%. Similar trends are seen at both test temperatures.

Statistical analyses also showed that there are no statistical differences in the power model constants due to changes in the gradation, aggregate source, or RAP source. Since the initial hypothesis was that this test should be primarily a function of binder properties, the lack of significant influence by the aggregate gradation and aggregate type was expected. It was originally thought that RAP sources from different regions of the country (Georgia and Minnesota) would produce measurable differences in the effective mix binder properties since different performance grades (PG) are used in the different regions. However, testing of the extracted RAP binders showed that there was little difference in the recovered, aged binder. Therefore, little change in the effective HMA binder is expected.

One of the potential uses for this test method is as an HMA contractor quality control (QC) test. QC samples, compacted for volumetric testing by a local HMA contractor, were used to evaluate this premise. Results show that both the stress relaxation modulus and the curvature coefficient for the unmodified asphalt binder used

by the contractor matched the expected values obtained during the initial laboratory study. This testing also showed the coefficient of variability in the stress relaxation modulus can be reduced from 30 to 18%, and from 15 to 7% for the curvature coefficient by testing each sample three times instead of only once.

ACKNOWLEDGEMENTS

I would like to thank Dr. Mary Gardiner for her guidance and assistance throughout this project. It is not often that one finds an advisor who always finds time for listening and help to solve all the little problems that are an unavoidable constant in any research work. I wish to acknowledge the help from the members of my committee, Dr. Dave Timm and Dr. Dan Brown for their help in correcting the dissertation. I would also like to acknowledge the assistance provided by the NCAT for the binder testing and TA Instrument for the loan of a new DSR.

Finally, I want to thank my wife, Annie, and my two sons, Sean and Kyle, for their patience, support, encouragement and love, which have kept me going during this project.

Style manual or journal used: The Chicago Manual of Style

Computer software used: Microsoft Word, Excel and PowerPoint

TABLE OF CONTENT

LIST OF TABLES

LIST OF FIGURES

Page

CHAPTER 1 INTRODUCTION

1.0 Introduction

Reclaimed asphalt pavement (RAP) is commonly used in combination with asphalt binders, or mixed with various percentages of new aggregates and asphalt binders to produce fresh hot mix asphalt (HMA) pavements. It can also be used in the lower pavement layers (i.e., binder and base layers) to provide improved layer support for traffic loads. However, limits on the amount of RAP are usually set because of the nation-wide implementation of the new Superpave binder specifications (Asphalt Institute, 1996). These specifications require the binder in the mixture to have rheological properties which will optimize long term pavement performance for a given set of environmental and traffic conditions. When RAP is added, the residual aged binder in the RAP mixes to some degree with the virgin binder. This produces a composite effective binder system with unknown material properties and hence unpredictable pavement performance.

For the purposes of this research, effective binder refers to the combination of neat asphalt binder and RAP binder that governs HMA properties that are primarily a function of the HMA binder. These properties include, but are not limited to, HMA critical low temperature (i.e., thermal cracking) and resistance to rutting. Changes in

these properties are due to the incorporation of the stiffer, aged RAP binder into the effective binder of the mix.

The NCHRP 9-12 (Use of reclaimed asphalt pavement (RAP) in the Superpave design method) was recently completed (McDaniel et al., 2000). The researchers found that RAP should not be considered a "black rock" because significant blending occurs between the RAP and neat asphalt binders. Researchers recommended that blending charts using neat and recovered RAP binder properties be used to account for the RAP contribution to the total binder properties or conversely, to select a softer (lower grade) neat binder when RAP is used in lower quantities. In blending charts, a linear relation is assumed between the amount of recovered RAP binder in the combined binder and the grade of the combined binder. Unfortunately, those blending charts are used for the binder alone, not the complete mix (binder and aggregates).

To use blending charts, the RAP binder must be extracted, recovered and graded. The extraction of the binder from a mix can be done in different manners, but to be able to recover the binder and grade it afterwards, the extraction must be done with solvents. Those solvents are dangerous and the extraction process can alter the properties of the binder. In the recovering process, the binder is heated which results in making the binder stiffer than it was in the mix. The gradation of the recovered binder is done with a dynamic shear rheometer (DSR). The complete extraction, recovery grading process can take up to a week.

The primary hypothesis for this research is that the tensile stiffness of mixtures within the linear viscoelastic range is primarily an indication of binder properties. Changes in mixture stiffness due to the inclusion of RAP in the mixture should therefore

reflect the contribution of the RAP binder to effective (combination of both neat and RAP binder) binder content. Using an indirect tension stress relaxation test rather than either tensile strength or a tensile creep test allows for the direct application of general linear viscoelasticity theory for predicting the dynamic (oscillatory) response. Therefore, the mixture test results can be theoretically converted into predictions of dynamic results as used in Superpave binder specification.

1.1 Objectives

The main hypothesis for this research is that the tensile properties of compacted HMA mixes will be governed by the properties of the asphalt binder, since this is the only component in the compacted sample that can withstand a tensile load. This hypothesis builds on the current low temperature indirect tensile strength creep test that is used to predict the critical low temperature at which the HMA pavement will exhibit thermal cracking. Thermal cracking has been shown to be primarily a function of asphalt binder properties (Carter, 2002). If this hypothesis can be applied to the results from a simplified indirect tensile stress relaxation test, then the properties of the asphalt binder can be evaluated by testing the compacted HMA samples rather than needing to extract, recover, and test the binder. Also, there should be a limited influence of gradation on the stress relaxation characteristics if the stress relaxation characteristics are mostly a function of only the asphalt binder properties.

The main objectives of this research were to:

- Develop and validate a simple, quick indirect tension stress relaxation test for assessing the asphalt binder properties using compacted HMA

samples that do not contain reclaimed asphalt pavement.

- Evaluate the effect of adding RAP to HMA mixtures on the stress relaxation characteristics of the mix.

1.2 Scope

Two experimental designs were used, one to accomplish each objective. The first experiment was developed to compare the asphalt binder stress relaxation properties to the HMA indirect tensile stress relaxation properties of the compacted HMA mixture. A parallel plate rheometer was used to develop shear stress relaxation master curves for two asphalt binders (PG 64-22, PG 76-22). These master curves were compared to indirect tensile stress relaxation master curves developed for the HMA mixtures prepared using the same two binders with either of two gradations. If the initial hypothesis is correct, and the indirect tensile stress relaxation test represents primarily binder properties, then there should be a good correlation between the two test results once shear modulus is converted to tensile modulus. A range of eight test temperatures was used to construct the master curves for the asphalt binder. Only two test temperatures were used to construct the master curves for the HMA mixes because of a time constraint. All tests, both asphalt binder and HMA, were done within the linear viscoelastic range.

The second experiment was designed to determine if the HMA indirect tensile stress relaxation characteristics are sensitive to changes in HMA mixture composition, such as those anticipated with various percentages of RAP. Once the HMA indirect tension stress relaxation test was validated as being representative of neat binder properties, a range of HMA mixes were tested and statistical analyses were used to assess

4

the influence of RAP on HMA mix properties. A Superpave gyratory compactor was used to prepare samples at mix design air voids (i.e., 4 percent) for two binder, two gradations, two aggregate types and two sources of RAP at one of five concentrations (0, 15, 25, 50, and 100 percent). The 100 percent RAP mixtures were used as a mixture representation of the recovered binder properties used in the blending charts recommended by McDaniel et al. (2000).

The potential for using this test as an additional QC test to monitor the consistency and grade of asphalt binder was evaluated once the test method was rigorously evaluated in the initial laboratory experiment. Compacted HMA samples prepared by a local HMA contractor for quality control (QC) testing of mix volumetric were collected and tested. The mixes, tested over one week of production, did not contain RAP; indirect tensile stress relaxation was conducted at only at two temperatures, 5 and 22°C.

1.3 Organization

The organization of this document is as follows:

Chapter 1 – Introduction of problem statement and initial hypotheses.

Chapter 2 – Literature Review

Chapter 3 – Theoretical Model Development

Chapter 4 – Materials and Methodologies

Chapter 5 – Results and Discussion

Chapter 6 – Conclusions and Recommendations

Chapter 2 provides background information on RAP, the different methods used to produce it, current practices for its design and use, and different problem associated with determining how to estimate the influence of the RAP binder on the effective HMA mix binder. Chapter 2 also includes a literature review that covers the influence of the addition of RAP to HMA mixes as evaluated in both the laboratory and field projects. Chapter 3 provides information regarding dynamic shear rheometer and viscoelastic models used in defining binders' behavior. It also establishes the fundamental relations between stress relaxation modulus and dynamic modulus. Chapter 4 documents all the materials used in this research program, sample preparation, sample compaction, and testing methodologies. Chapter 5 explains the relationship between dynamic shear modulus and stress relaxation tests on binder alone. The relationship between the stress relaxation for binder and for the mixes, with and without RAP, is also discussed in this chapter. The last sections in Chapter 5 present the results of the field study that uses the test method as a possible QC test during construction. Finally, Chapter 6 summarizes the results of the research program and suggests future work.

CHAPTER 2 LITERATURE REVIEW

2.0 Introduction

It has been well established that binder properties have a large effect on the properties of hot mix asphalt (HMA) mixes (Roberts et al., 1991). Binder viscosity needs to be sufficiently low at high temperatures to allow the material to be moved through the HMA plant. It also needs to be sufficiently stiff at the average maximum high in-service temperature so that load-induced deformation (rutting) is minimized. At the same time, the binder needs to be flexible (ductile) at cold temperatures so that thermal cracking is minimized by the material's ability to dissipate stresses through deformation.

The performance graded (PG) asphalt binder specification was a product of the Strategic Highway Research Program (SHRP) program (circa 1993) and was developed to evaluate fundamental properties of binders under the expected local environmental conditions. This specification incorporates three rheometers for defining key asphalt binder properties over a wide range of temperatures. A concentric cylinder rheometer at $135^{o}C$ is used to set a maximum viscosity for workability (i.e., pumpability). A dynamic shear rheometer (DSR) is used to define the complex shear modulus (i.e., viscoelastic stiffness) at both high (summer) and intermediate (spring/fall) in-service temperatures. A bending beam rheometer evaluates cold (winter) temperature stiffness and rate of deformation.

Ideally, the PG binder grading specification should be used to evaluate the binder properties of reclaimed asphalt pavement (RAP)-modified HMA as well as the blend of virgin and RAP binder that will form the effective binder in the final RAP mix. However, current methods for estimating the influence of RAP on binder properties requires that the aged asphalt in the RAP be solvent extracted, hot-recovered from the solvent, and tested. These results, mathematically combined with the results with virgin asphalt test results, are used to estimate composite binder properties. The amount of RAP that is actually incorporated into the effective HMA binder cannot currently be assessed.

This chapter is separated into four sections. First, a summary of RAP production and how it is used in new mixes is presented. Second, a brief summary of the current practice for estimating binder properties of HMA with RAP is shown as well as problem with the current practice. The third section shows the influence of the addition of RAP in a new mix and how that influence is measured.

2.1 Reclaimed Asphalt Pavement (RAP)

RAP is the acronym for Reclaimed Asphalt Pavement. "Recycled" rather than "Reclaimed" Asphalt Pavement is also an often-used term. RAP is produced when a paved road is milled during rehabilitation; it is not a new process. The first documented case of hot in-place recycling was done in the 1930's (ARRA 2001). The interest in asphalt recycling has increased in the 1970's because of the petroleum crisis and because a large scale milling machine was developed in 1975.

The Federal Highway Administration (FHWA) reports that around 91 million metric tons of pavements are milled every year in the USA. About 80 percent of that is

reused in new roads, road bed, shoulders and embankments (APA 2004) saving taxpayers almost $300 million annually (Eighmy and Magee 2001). Each state has different rules as to how much RAP is allowed in the different layers of the pavement. The percent used ranges from 0 to 70% in the base course, the binder course or the surface course (Banasiak 1996). A complete table showing the percentage allowed for each state is shown in Appendix A.

2.1.1 Candidate Projects for Recycling

Almost any HMA rehabilitation project that requires an overlay is a candidate for recycling. However, there is some limitation to the process. For example, if the distressed pavement layer is very thin, the milling machine may break it into chunks which would need additional crushing before being reused. In this case, it may be more economical to simply put an overlay on top of the existing surface (Roberts et al., 1991).

Also, if the aggregates in the existing pavement do not meet the materials specifications for the new mix, the old pavement will be simply discarded or used in other projects in the lower layers. This will be done if there is too much fine material, if the aggregate tends to polish or if it breaks too easily.

Pavement recycling is used to removed rutted or oxidized pavements or to correct the profile of the road. If the problem of the pavement is structural, recycling is not the solution.

2.1.2 Asphalt Recycling Methods

There are four main asphalt recycling methods: Hot recycling, Hot In-Place recycling

(HIR), Cold Recycling (CR) and Full Depth Reclamation (FDR). The information in this section comes from ARRA (2001) unless stated otherwise.

2.1.2.1 Hot Recycling

Hot recycling is the most popular asphalt recycling technique in the world. In the USA, over 50 millions tons of RAP are generated annually by State Highway Agencies and around 33 percent of that is used in hot recycling (APA 2004). Hot recycling is the mixing in a plant of the RAP and new aggregates, binder and sometimes recycling agent. The amount of binder contained in the RAP and the viscosity of the recycled binder is an important factor in the choice of the virgin binder. Once the new mix is produced, it is placed and compacted with conventional HMA equipment.

2.1.2.2 Hot In-Place Recycling (HIR)

In hot in-place recycling, the pavement is softened by heating then scarified. The recycled HMA can be used by itself, but often new aggregates and binder are used to correct the mix composition and volumetric. Oxidized binder can be rejuvenated during HIR by adding a recycling agent in the mixing process.

Since HIR is done in one step, the traffic disruption is very limited. However, the maximum treatment depth is around three inches. If the distress in the pavement layers is deeper than this depth, another method of recycling will be necessary.

2.1.2.3 Cold Recycling (CR)

Cold recycling can be done in place or at the plant. In cold recycling, the asphalt pavement is removed without the use of heat. Cold in-place recycling processes often mix the RAP with an emulsion, then place and compact the mix. This new mix can be used as a stabilized base, or, less frequently, as the wear course on low volume roads. The in-plant cold recycling process is the same except that the RAP in stocked and mixed only when needed. CR is usually done on the top two to four inches of pavement.

2.1.2.4 Full Depth Reclamation (FDR)

FDR is a cold in-place recycling technique that pulverizes the top four to twelve inches of materials. The pulverized material usually includes the asphalt layer and a part of the base layer. The reclaimed pavement is then mixed and more materials can be added (aggregates, binder, etc.) before being placed. This new material is considered a treated base; it is compacted and graded before being covered by a new asphalt pavement layer.

2.2 Current Practices for Estimating Binder Properties of HMA with RAP

Selection of the virgin asphalt PG grade depends on the quantity of RAP added. According to McDaniel et al. (2000), if less than 15% of RAP is used, there is no need to change the binder grade. If between 15% and 25% of RAP is used, the virgin binder grade is commonly decreased by one grade (6°C) on both ends (e.g. a PG 64-22 is changed to a PG 58–28). If more than 25% of RAP is used, then the RAP binder needs to be extracted, recovered and graded using the performance-graded binder tests. This information, along with the same test information for the new binder is then used to construct blending charts.

11

Other guidelines based only the recovered RAP binder properties were presented by McDaniel et al. (2001). These guidelines (Table 2.1) are a more precise since the quantity of RAP allowed is based on the recovered binder properties which are different with every RAP stockpile. This table indicates that a warmer lower temperature grading of the RAP binder results in a decrease in the amount of RAP that can be used in the mix. That is, a grading of -22°C allows the use of at most 20% RAP; when the grading of the RAP is -10°C, only 10% at most RAP can be used.

Table 2.1: Guidelines for binder selection for RAP mixtures (McDaniel et al., 2001)

	RAP Percentage		
	Recovered RAP Grade		
Recommended Virgin Asphalt Binder Grade	**PG xx-22 or lower**	**PG xx-16**	**PG xx-10 or higher**
No change in virgin binder selection	< 20%	< 15%	< 10%
Select virgin binder one grade softer than normal (ex.: PG 58-28 instead of PG 64-22)	20-30%	15-25%	10-15%
Follow recommendations from blending charts	>30%	>25%	>15%

2.2.1 Blending Charts

The blending charts are used to determine the percentage of RAP needed to produce a mix with a specific PG binder grade when the percent of RAP to be used is more than 25% (McDaniel et al., 2001). Although it can be used for any percentage of RAP, the approach requires significant testing and time in order to obtain results so it is usually limited to only the higher percentage of RAP mixes. There are two ways to use the blending charts:

- A known percentage of RAP to be used and the virgin binder grade needs to be selected to achieve a specific blended binder grade.

- A known virgin binder grade and the percentage of RAP that can be used to achieve a specific blended binder grade needs to be selected.

The charts are built following the Superpave grading specification. To build a blending chart, the recovered binder is tested with a dynamic shear rheometer (DSR) and a bending beam rheometer (BBR) in order to estimate the PG grading of the RAP binder. The same tests are done for the virgin binder. Two charts need to be constructed, one for the high temperature properties (i.e, DSR results) and one for the low temperature properties (i.e., BBR results). For example, if the grade of the recovered binder is found to be PG 82-10 and the grade of the virgin binder is PG 58-28, the blending chart for high temperature (Figure 2.1) shows that between 25% and 50% of RAP can be added to achieve a blended grade of PG 64-22. The low temperature blending chart (Figure 2.2) shows that a maximum of 33% of RAP can be added to achieve a PG 64-22. So anywhere between 25% and 33% would be appropriate. Instead of using the graphical solution, one can use the following equation:

$$\% RAP = \frac{T_{blend} - T_{virgin}}{T_{RAP} - T_{virgin}}$$ Eq. 2.1

where:

$\% RAP$ is the percentage of RAP expressed in decimal

T_{blend} is the critical temperature of the blended asphalt binder

T_{virgin} is the critical temperature of the virgin asphalt binder

T_{RAP} is the critical temperature of the recovered RAP binder
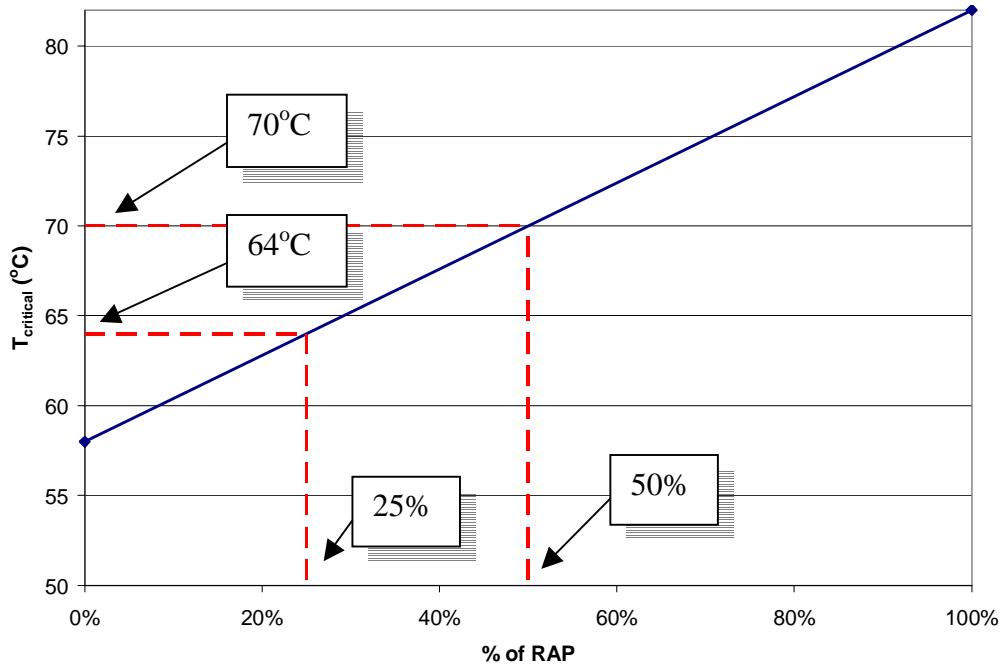
Figure 2.1: Example of blending chart for high temperature
(% of RAP unknown)
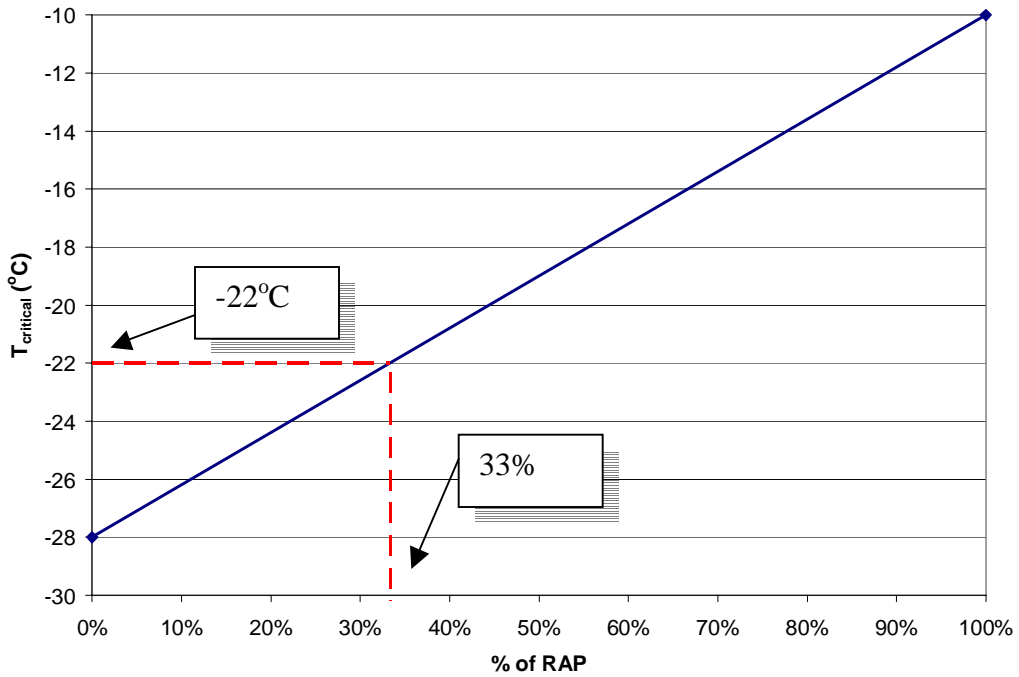
Figure 2.2: Example of blending chart for low temperature
(% of RAP unknown)

Even though the Superpave method recommends using both original and rolling thin film oven (RTFOT) high temperature blending chart, usually only the original binder property blending chart is used to avoid running the time consuming RTFOT testing (ARRA 2001).

2.3 Problems with Current Practice

Every method that can separate the binder from the aggregates in an HMA uses a solvent such as 1,1,1 trichloroethane (TCA), trichloroethylene (TCE), methylene chloride, or toluene. The solvent removes the binder from the aggregate, and by distillation, the binder is separated from the solvent. The first problem with this practice is that the solvent does not completely remove the binder from the aggregate (Cipione et al., 1991). After a TCE extraction, there can be up to 2% of binder left on the aggregate (Peterson et al., 1982). The binder that is not extracted represents a part of the binder that is strongly adsorbed on the surface of the aggregate. Because this part of the binder is not present in the extracted binder, it is possible that the properties determined for the extracted binder do not represent the actual RAP binder properties (Peterson 1984).

The second problem with the use of solvent is that the binder typically becomes stiffer after extraction (Burr et al., 1991). This hardening appears in all solvent extraction methods, but to a lesser extent when cold extraction processes are used as compared to hot extraction methods. Once again, the hardening of the binder will results in binder properties different than the actual binder properties in the mix.

Another problem lies in the fact that solvent extraction is expensive. The price of the solvent is not too high, but the cost associated with disposing of the waste is high (Behrens et al., 1999). When TCE is used, the cleaned aggregates are considered

hazardous waste because the flash point is under 140°F (McGraw et al., 2001). The flash point is the temperature at which the vapor of the heated material ignites in the presence of a spark or an open flame (Roberts et al., 1996). There are also health problems associated with the use of solvent. TCE for example, has been proven to causes cancer in mice and rats and is suspected of causing cancer in humans (Fialka 2004).

Finally, there is a large variability in the properties of the recovered binders. In a research by Stroup-Gardiner and Nelson (Stroup-Gardiner and Nelson 2000), it was shown that the within-laboratory variation for binder testing is about 23 to 30% and about 38 to 45% between-laboratory. This variation can be explained by the problems noted above. In addition, some solvent may remain in the binder after recovery, which may also alter the properties (Collins-Garcia et al., 2000).

2.4 Influence of the Addition of RAP in a New Mix

Previous research has shown that tests to evaluate the effect of the addition of RAP in a new mixture can be used to adjust the new HMA mix design. These studies concentrate on evaluating changes in key mix properties that are related to pavement performance such as fatigue (Huang et al. 2004) and mix stiffness. The fatigue tests done by Huang et al. (2004) were done in indirect tension (IDT). Indirect tension tests are easy to perform, but they are more complicated to analyze due to the complicated stress contours within the sample.

The tensile strength (ITS) and the toughness index (TI) have also been used in that research (Huang et al., 2004). TI is a parameter describing the toughening characteristic in the post-peak stress region. A perfectly plastic material will have a TI of 1 and an ideal brittle material will have a TI of 0, therefore HMA with and without RAP

16

will have TI values between these two limits. This research showed that there is no significant difference in ITS and TI between mixes containing 0 or 10% of RAP. There is also no significant difference between mixes containing 20% to 30% of RAP. However, between 0 and 20% of RAP, ITS increase significantly and TI decrease significantly (Huang et al. 2004). If related to fatigue, this would mean that mixes containing at least 20% of RAP would have the potential to absorb more strain energy before they start to fail but after failure (cracks), the specimen would fail faster (lower post-failure tenacity).

As for the effect of the addition of RAP to the complex modulus, it was found that the complex modulus increases with the percentage of RAP (Daniel et al. 2004 and Sondag et al. 2002). According to Sondag et al. (2002), the source of RAP also has an influence on the complex modulus since different RAP sources have different binder properties. The phase angle, measured during the complex modulus test, decreases with the addition of RAP (Sondag et al. 2002). The rate of decrease is high between 0 and 15% of RAP and much smaller between 15 and 40%.

It was also been found that the resilient modulus tends to increase with the addition of RAP (Sargious and Mushule 1990, Sondag et al. 2002 and Garg and Thompson 1996). On the other hand, Kandhal et al. (1995) has shown that the difference in resilient modulus between an HMA with virgin material and a mix containing RAP is often not statistically different. This is probably due to the fact that binders with lower viscosity were used when large amount of RAP was used. It could also be a function of the variability in the test method.

2.4.1 HMA Modulus

There are currently two main methods to determine the modulus of asphalt concrete; a dynamic or repeated load axial compression test and a dynamic or repeated load diametral indirect tension test (IDT). The main difference between these two tests is the state of stress in the specimen (Kim et al. 2004). In the axial compression test, there is a uniaxial state of stress, while the diametral configuration produces a biaxial state of stress. Therefore it is more complicated to calculate the modulus using the IDT test than the axial compression test.

The results from IDT and compression tests are not always in good agreement when testing HMA because this material can have different properties in tension as compared to compression. In fact, the modulus calculated from both methods is only similar at low temperature (Khanal et al., 1995). The difference in results from the two test methods can be explained by the fact that at low temperature, the binder is stiff and does not allow the movement of the aggregates as well as it does at higher temperatures. Both tests are more representative of the binder properties than the aggregates properties when done at low temperatures. It should be noted that at room temperature and higher, compression test results represent more of the aggregates properties than the binder properties. This is because in compression, the contact between the aggregates (i.e., aggregate interlock) that mainly control the strain. In a tension test, the aggregate interlock does not have a big effect because the only thing keeping the aggregate particles from separating is the binder. The modulus calculated from a compression test can be 35 to 45% higher than the modulus calculated from the indirect tension test (Tayebali et al., 1995).

Even though IDT tests are simple to perform, one needs to know or to determine Poisson's ratio in order to calculate a precise modulus (Roque and Buttlar 1992). Poisson's ratio is usually assumed to be 0.35, but it changes depending on the mix, the test temperature and the frequency of the test (Tayebali et al., 1995). It is generally accepted in HMA analysis that Poisson's ratio is assumed to be 0.2 at temperatures lower than 10°C, 0.35 between 10 and 30°C, and 0.5 above 30°C. Assumptions are made about Poisson's ratio because this property is very difficult to measure during testing; problems are related to the sensitivity of sensors at very low strain measurements, equipment vibrations, gauge mount slippage, and the localized but high compressive zone directly under the loading strips (Wallace and Monismith 1980).

In an IDT test, the horizontal and vertical strain can be measured externally or internally. When the vertical displacement is measured by an LVDT on the ram, it is called external. The horizontal strain is then calculated using an estimated Poisson's ratio. An internal measurement uses strain gages glued to the center of one or both flat faces of the sample. The main disadvantage of using external measurement is that the strain near the point of contact on the specimen will be taken into account in the calculation even if it is not representative of the failure plane (Roque and Buttlar 1992). External measurement will also measure any rocking of the samples. Internal measurements will measure only what happens in the center part, but the strain gages are so small that any segregation in that section of the sample will results in erroneous results (Wallace and Monismith 1980).

In the IDT creep test used to estimate thermal cracking potential, the master creep compliance curve is transformed in the master relaxation modulus curve by a Laplace transformation, which is then used to compute the thermal stresses in the pavement

according to a constitutive equation (Lytton et al. 1993). The indirect creep test was preferred to the indirect stress relaxation test because, according to Baumgaertel and Winter (1989), it is easier to conduct and more reliable than the relaxation test. One of the reasons that makes the relaxation test more complicated is the need to reach a precise strain in a very short time (Menard 1999). Another reason given for the preference of creep testing over relaxation testing is that creep tests can be more useful to engineers and designers (Nielson and Landel 1994).

2.5 RAP Mix Field Applications

RAP has been extensively used in projects all over USA and Canada. In most cases, the pavement constructed with RAP had mechanical behavior comparable to pavement made with virgin mixes (McDaniel et al. 2002, Emery 1993, Kandhal et al. 1995, Garg and Thompson 1996, Hossain et al. 1993, Tam et al. 1992, Paul 1996, Larsen 2003, TFHRC 2004 and Cosentino et al. 2003). RAP is now used in almost all 50 states in the base, the binder course, and the surface course and as noted before, each state has their own specifications regarding the amount of RAP that can be used and where it can be used (Appendix a, Table A1) (Basaniak 1996).

Historically, the amount of RAP that could be added in a mix was limited by the heating capacity of the equipment (Shoenberger et al. 1995). RAP was initially added with the aggregate, which created problems when the old binder came into contact with the open flame. As technology improved, drum plants were modified with a collar further down the drum and away from the flames for the addition of the RAP.

When RAP is used in the base material, it was found that the California Bearing Ratio (CBR) is lower compared to a base made of crushed aggregate (Enery 1993, Garg and Thompson 1996, Cosentino et al. 2003). Taha et al. (1999) hypothesize that the CBR is lower with the addition of RAP when compared to virgin aggregate because the RAP binder creates a slip plane between the aggregate, which facilitates the movement of the aggregates.

In any cases reported in these studies, there was no difference in rutting between HMA overlays with or without RAP. Fatigue cracking was found to increase when RAP was used in the wearing course (Paul 1996). There is some evidence that if 20% RAP or more is used in the wearing course, the viscosity of the combined binder will likely increased over a limit (12 000 poise at 60°C), above which pavements tend to crack. However, Hossain et al. (1993) observed that mixes used as wearing course containing 50% RAP have a lower rate of fatigue crack increase than virgin mix. It should be noted that the virgin mix contained an AR-8000 binder and that the recycled mix, which has 0.5% more asphalt binder, contained an AR-4000 binder.

According to Tam et al. (1992), if less than 50% of RAP is used, the amount of thermal cracking should be limited. In this study, thermal cracking was directly related to the penetration of the binder. If the penetration of the recovered combined binder (virgin + RAP) is under 20 dmm, over 20 000m/km of crack length can be expected (Tam et al., 1992). This means that the pavement will be completely disintegrated due to thermal cracking. In another case documented by Sargious and Mushule (1991), mixtures containing 45% of RAP were found to crack at colder temperature than mix without RAP. The softer virgin binders used in with RAP mixes (400/500 penetration grade in

the RAP mixes and 150/200 penetration grade in the virgin mixes) may be the reason for the lower amount of cracking seen in these studies. Larsen (2003) reported that in a case of a project in Connecticut, the only differences between pavement made with a wearing course containing 20% RAP and pavement made with virgin mixes came from the layers underneath. In that project, there were no significant differences in any types of cracking or in rutting between virgin and RAP mixes after five years of monitoring.

2.6 Summary

The current practice to use RAP in new mixes include the extraction of the binder in the RAP and its gradation. Unfortunately, the extraction process requires solvent that can be a health hazard, that are expensive to get rid of, and that can change the binder properties. The amount of RAP to be used is set depending on the PG grade of the RAP binder, the PG grade of the virgin binder, and the PG grade needed from the combined binders. Blending charts are currently used to evaluate the effect of the RAP binder on the PG grade of the combined RAP binder. Blending charts assume that there is a linear relation between the amount of RAP binder included in the combined binder and the change in PG grade.

The addition of RAP to a mix makes the resulting HMA stiffer. An addition of 15 to 20% of RAP is enough to increase the complex modulus and to alter the fatigue characteristics. Depending upon the PG grade of the virgin binder and the pavement structure, the fatigue properties may improve or deteriorate. In some cases, it has been shown that only 20% of RAP in the wear course is necessary to increase fatigue cracking. This literature review emphasizes the need to be able to evaluate the actual HMA mix

properties in order to select the most appropriate percentage of allowable RAP, or to

select the PG grade of virgin binder to use with a preselected percentage of RAP.

CHAPTER 3. THEORETICAL MODEL DEVELOPMENT

3.0 Introduction

In polymer science, the relation between dynamic modulus, creep modulus and relaxation modulus has been well established. Since asphalt binders are considered to behave like short-chain polymers (i.e., oligomers), the same relations can applied. Lately, the relaxation spectrum has been used to determine the zero shear viscosity of binders (Rowe and Pellinen 2003).

In this chapter, the instrumentation used to analyze the binder rheology is described, the mathematical model used to represent the binder behavior, and the relation between the dynamic and the stress relaxation modulus are explained.

3.1 Dynamic Shear Rheometer (DSR)

The main advantage to using the DSR to determine binder stiffness is that the viscoelastic (i.e., time-temperature) properties of the material can be considered. The DSR is a parallel plate rheometer that is set up by sandwiching an asphalt sample between two circular plates. The asphalt is sheared by the oscillatory movement of the upper plate at a speed of 10 rad/s (frequency set by PG specification). The applied shear stress is a sinusoidal signal oscillating around zero. The actual test temperatures are based on the anticipated in-service temperature in which the binder will be used.

To correctly describe the behavior of a binder, the complex shear modulus, G*, and the phase angle, δ, are needed. G* is the maximum shear stress divided by the maximum shear strain of the oscillatory signal. The phase angle is the time lag between the stress and strain signals. A perfectly elastic material has a phase angle of zero since the strain follows the stress perfectly. With a purely viscous material, there is a 90° difference in the position of the stress and strain signals. Materials that exhibit a combination of both elastic and viscous behavior are call viscoelastic and have a phase angle somewhere between 0 and 90° (Roberts et al. 1996).

Two parameters measured with the DSR are used in the PG binder specification to quantify binder properties for adequate pavement performance with regards to rutting resistance and fatigue resistance (Roberts et al. 1996). For rutting, the binder must be stiff (high G*) and elastic (low phase angle) to resist the shear stresses from traffic loads and to have as little permanent deformation as possible. For fatigue resistance, the binder should be soft (i.e., low G*) and elastic (i.e., low phase angle) to allow the HMA layer to flex without cracking after a number of repetitive loading cycles.

3.1.1 DSR Geometry

The three most commons geometries used with a DSR are the parallel plate, cone and plate and the concentric cylinder (Macosko 1994) (Figure 3.1). These three geometries all have advantages and disadvantages.

a) Cone and
   plate

b) Concentric
   cylinder

c) Parallel
   plate
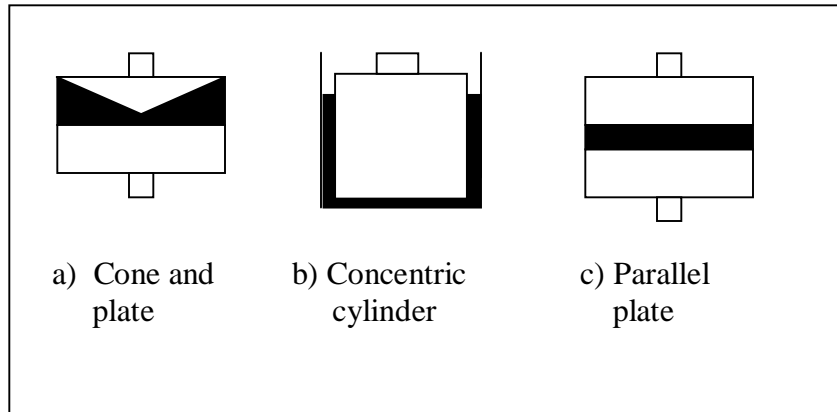
Figure 3.1: DSR Geometry

3.1.1.1 Cone and Plate

The cone and plate geometry (Figure 3.1a) is used with sample with submicron size particles. Samples with particle matter in them, such as binder mastics, should not be tested with the cone and plate geometry since the solid particles will tend to migrate to the apex of the cone and get jammed. This would results in erroneous results since one of the underlying assumptions for this test is that the material is homogenous (TA 2003). The main advantage of the cone and plate geometry is the fact that the shear strain and shear rate are constant in the sample (Macosko 1994).

3.1.1.2 Concentric Cylinder

The concentric cylinder (Figure 3.1b) is for testing materials with a low viscosity that can be poured into the bottom cylinder. In the HMA industry, concentric cylinder rheometers are used to evaluate the high temperature viscosity of the binder. A maximum viscosity is set in the PG specification to make sure that the binders can be pumped during HMA production. High temperature viscosity values for at least two temperatures can be used to set the laboratory mixing and compacting temperatures.

3.1.1.3 Parallel Plate

The parallel plate geometry (Figure 3.1c) produces a shear strain that is not homogeneous; it depends on both the radial and vertical position within the sample. Since the calculation of shear stress and strain use equations for a cylindrical geometry, care needs to be taken during sample preparation to make sure that the sides of the sample are perpendicular to the upper and lower plates. This configuration can be used to test materials with discrete particles in the binder, however there is a general guideline that indicates the gap between the plates needs to be no less than 10 times the diameter of the largest discrete particle (TA 2003).

3.1.2 Stress and Strain Calculations Using Parallel Plate

The sample used with the parallel geometry is usually 1 or 2 mm thick and the plates have 8 or 25mm in diameter when testing asphalt binders (Kennedy et al., 1994). The diameter of the plate is chosen depending on the test temperature since the DSR has a limited torque capacity. A smaller diameter of the cylindrical geometry is needed with a stiffer material or a colder test temperature.

The shear stress is calculated by dividing the applied force, the torque in this case, by the area on which the force is applied:

$$\tau = \frac{2T}{\pi r^3} \qquad \qquad \text{Eq. 3.1}$$

where:

τ = shear stress (Pa)

T   = torque (N-m)

r   = radius (m) (Figure 3.2)

27

Also, by definition, the shear strain is the deformation caused by forces that produce an opposite but parallel sliding motion of the body's plane. In the DSR test with parallel plate, the shear strain is calculated by dividing the angular movement by the thickness of the specimen:
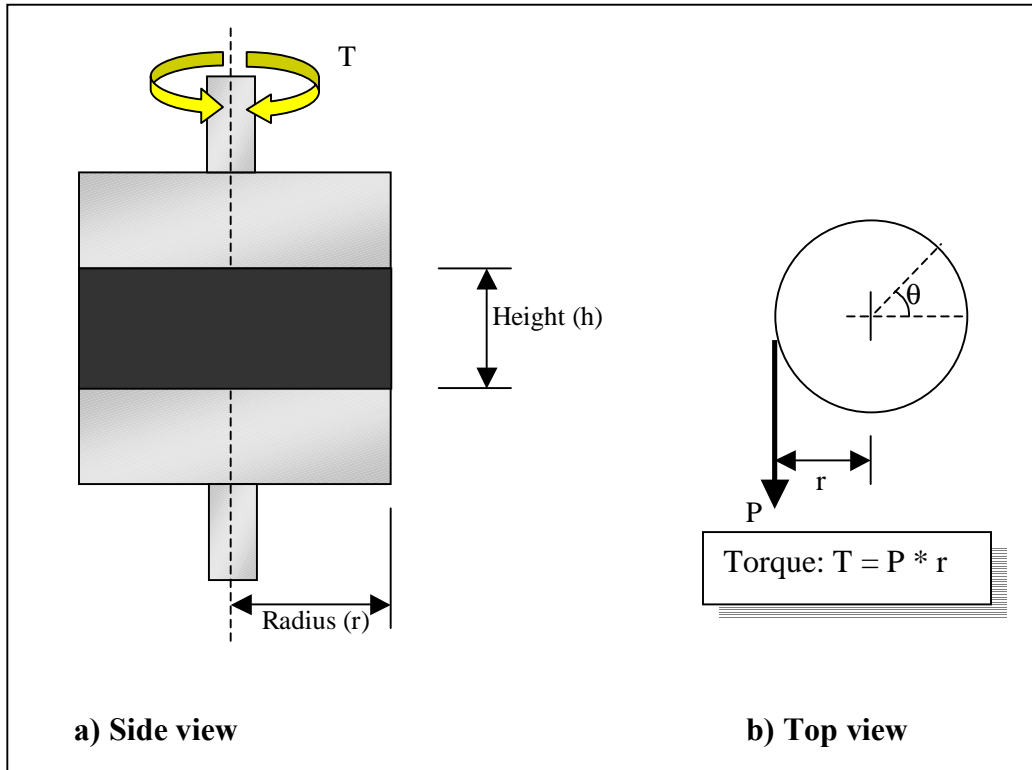
Figure 3.2: Parallel plate geometry

$$\gamma = \frac{\theta\, r}{h}$$ Eq. 3.2

where:

γ   = shear strain (mm/mm)

θ   = angular displacement (rad)

r   = radius (mm)

h   = thickness (distance between plates) (mm)

The shear strain commonly used is the shear strain measured at the edge of the plate (Kennedy et al. 1994). The angular displacement is measured by relative displacement of the upper and lower shaft. With the stress and the strain, it is possible to calculate a modulus. If the stress is maintained constant, it is called the creep modulus. If it is the strain that is held constant, it is called the relaxation modulus.

3.2 Viscoelastic Models

Theoretically, relaxation modulus can be used to predict dynamic modulus. The following section shows how the equations from each part are derived so the results from one test can be compared to the other.

3.2.1 Basic Equations

When a purely elastic body without any inertial effect is subjected to an instantaneous stress, it responds with an instantaneous strain; it is the Hooke law (Aklonis et al., 1983). For a shear displacement, the equation is:

$$\tau = G\gamma \qquad \text{Eq. 3.3}$$

Where:

τ = stress (Pa)

γ = strain (mm/mm)

G = shear modulus (Pa)

On the other hand, a fluid with no elastic behavior but simple linear viscous behavior will obey Newton's law (Menard 1999):

$$\tau = \eta \frac{d\gamma}{dt}$$
<div align="right">Eq. 3.4</div>

Where:

η = viscosity (Pa.s)

$d\gamma/dt$ = shear strain rate (s^{-1})

$\mathbf{G}$ for elastic materials as well as $\mathbf{\eta}$ for viscous materials are proportionality constants. The biggest difference between those two expressions is the fact that there is a time dependency for a fluid.
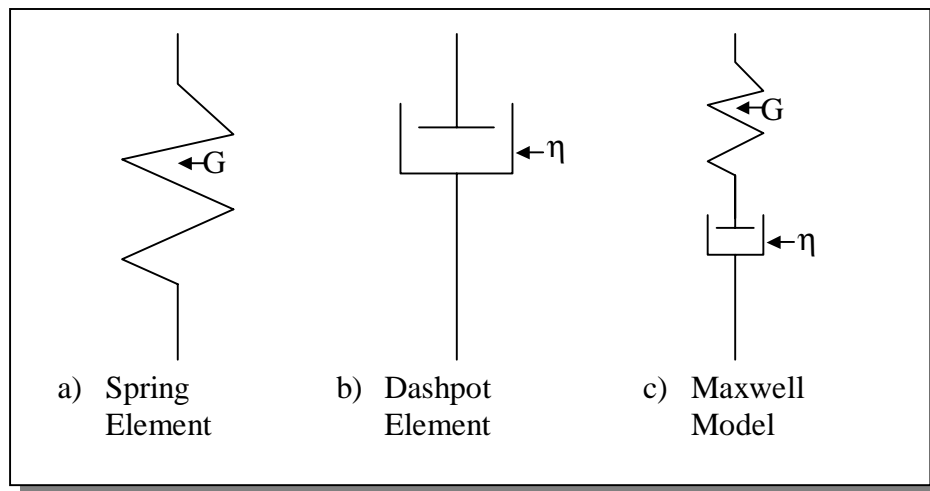
Figure 3.3: Spring and dashpot element and the Maxwell model

3.2.2 Relaxation Modulus Modeling

The Maxwell model provides a mathematical combination of elastic (spring, Figure 3.3a) and viscous (dashpot, Figure 3.3b) material behavior. The individual components are in series (Figure 3.3c). In a Maxwell model, the stress is the same in the two elements since they are in series, but the strain differs.

Since **G** and η are two proportionality constants, the relationship between the two is (Haddad 1995):

$$\eta = \lambda G \qquad \text{Eq. 3.5}$$

where:

λ = relaxation time of the element (a constant)

To calculate the behavior of a material with the Maxwell model, the equation of motion of the Maxwell model is used. In this equation, the derivative of the strain as a function of time is the result of the immediate elastic behavior (first part on the right side) and the viscous behavior (second part on the right side):

$$\frac{d\gamma}{dt} = \frac{1}{G}\frac{d\tau}{dt} + \frac{\tau}{\eta} \qquad \text{Eq. 3.6}$$

In a stress relaxation experiment, an instantaneous strain of γ_o is imposed to the sample and the change in stress with time is recorded ($\tau(t)$) (Rosen 1993). Since the strain is theoretically an instantaneous strain, $d\gamma/dt = 0$ after the load application, so equation 3.6 becomes:

$$0 = \frac{1}{G}\frac{d\tau}{dt} + \frac{\tau}{\eta} \quad or \quad -\frac{\tau}{\eta} = \frac{1}{G}\frac{d\tau}{dt} \qquad \text{Eq. 3.7}$$

If equation 3.5 is combined with equation 3.7, the result is:

$$-\frac{\tau}{\lambda G} = \frac{1}{G}\frac{d\tau}{dt} \qquad \text{Eq. 3.8}$$

This equation can be simplified to:

$$\frac{d\tau}{\tau} = -\frac{dt}{\lambda} \qquad \text{Eq. 3.9}$$

The integration of that equation from a time **0** to a time **t** is:

$$\int_{\tau_0}^{\tau_t} \frac{d\tau}{\tau} = -\frac{1}{\lambda} \int_{t_0}^{t=t} dt \quad \Rightarrow \quad \ln \tau(t) - \ln \tau(0) = -\frac{t}{\lambda} \qquad \text{Eq. 3.10}$$

Equation 3.10 can be transformed in an exponential and then both sides of the equation are divided by γ_0.

$$\ln \frac{\tau(t)}{\tau(0)} = -\frac{t}{\lambda} \quad \Rightarrow \quad e^{-\frac{t}{\lambda}} = \frac{\tau(t)}{\tau(0)} \quad \Rightarrow \quad \tau(0) e^{-\frac{t}{\lambda}} = \tau(t) \quad \Rightarrow \quad \frac{\tau(0) e^{-\frac{t}{\lambda}}}{\gamma_0} = \frac{\tau(t)}{\gamma_0} \qquad \text{Eq. 3.11}$$

The right side of equation 3.11 is the stress relaxation modulus and on the left side, the shear modulus is multiplying the exponential. This can be simplified as:

$$G_0 e^{-\frac{t}{\lambda}} = G(t) \qquad \text{Eq. 3.12}$$

It should be noted that the larger λ is, the slower the stress will relax (Wineman and Rajagopal 2000). This means that the relaxation time is a measure of how quickly the stress relaxes.

3.2.2.1 Maxwell-Wiechert model

Unfortunately, for the Maxwell model to represent experimental test results, a series of relaxation time and elastic modulus have to be used (figure 3.4). This series, called a Prony series (Wineman and Rajagopal 2000). Equation 3.12 becomes:

$$G(t) = \sum_{k=1}^{k=n} G_k e^{-\frac{t}{\lambda_k}} \qquad \text{Eq. 3.13}$$

In Figure 3.4a, only one relaxation time and modulus is used in the model. In 3.4b, five different relaxation time and modulus are used to better fit the experimental data.

According to Tsai et al. (2004), 12 couples of relaxation time and modulus should be used to have a good model. The sum in equation 3.13 can be represented as a series of Maxwell elements placed in parallel (Figure 3.5) (Barnes 2000). This model is called the Maxwell-Wiechert model (Aklonis 1983).

To obtain the relaxation time and modulus for this model, a relaxation time that is evenly spaced is chosen and the modulus is determined with a linear regression equation that minimizes the least square. The relaxation time used in the Maxwell model for the relaxation experiment can then be used to simulate the dynamic modulus. The relaxation time is the constant that links the two types of experiment.

It should be noted that the Maxwell model is suitable for relaxation experiments on polymer material, but not for the creep experiments. Also, the Maxwell model predicts that the stress will relax to zero over a long period of time; this is not really the case with polymer (Young et al., 1994).

All the equations shown above were written for shear experiments. The same equations are valid for a linear relaxation experiment. In terms of axial loading stress, strain, and modulus, Equation 3.13 becomes:

$$E(t) = \sum_{k=1}^{k=n} E_k e^{-\frac{t}{\lambda_k}}$$

Eq. 3.14

where:

E   = elastic modulus (Pa)
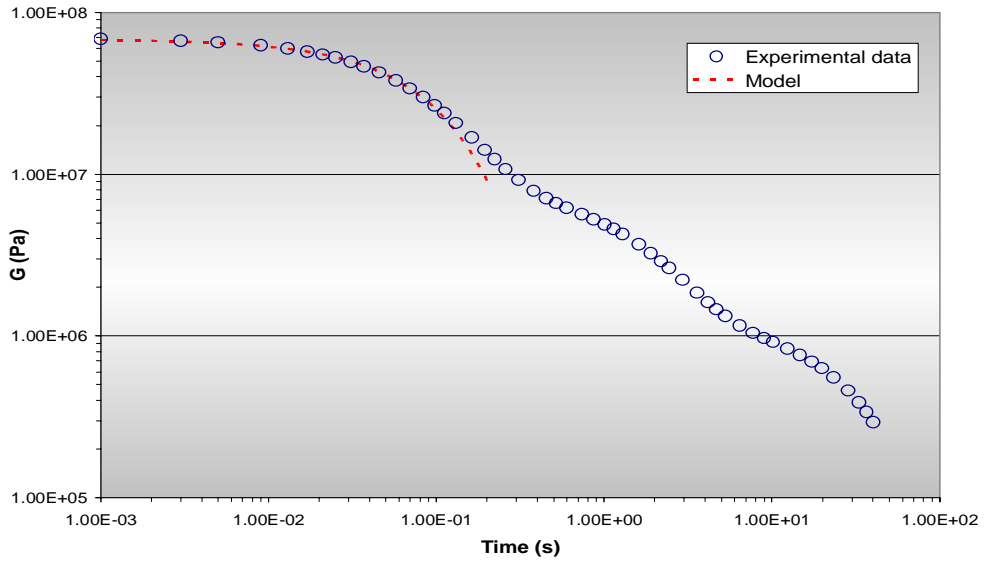
a) Curve fitting with only one exponential
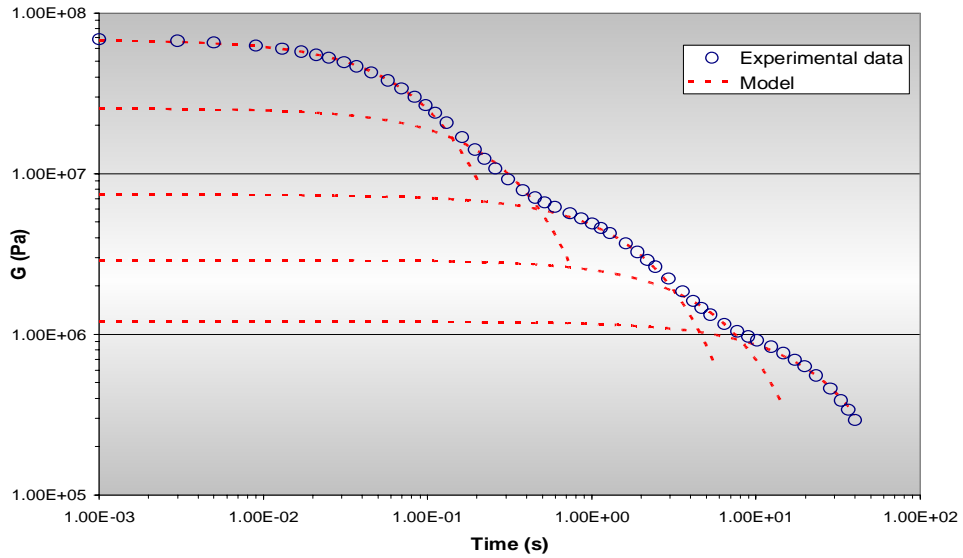
b) Curve fitting with a five constant exponential model

Figure 3.4: Comparison of experimental data with model
(Based on Macosko 1994)
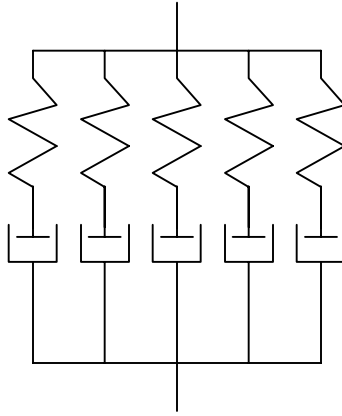
Figure 3.5: Maxwell-Wiechert model

Equations 3.13 and 3.14 should not be used when trying to model the behavior over a wide time because these estimates will get less and less precise the longer the experiment lasts (Nielsen and Landel 1994).

3.2.3 Dynamic Modulus

When a sinusoidal oscillation test in shear strain control is done, the strain and the stress can be written as (Figure 3.6):

$$\gamma = \gamma_0 \sin \omega t \qquad \text{Eq. 3.15}$$

$$\tau = \tau_o \sin(\omega t + \delta) \qquad \text{Eq. 3.16}$$

where:

γ_o, τ_o = amplitude of shear strain and stress

δ = phase angle

ω = angular frequency (2π times the frequency in Hz)

The stress wave can be separated in two different waves:
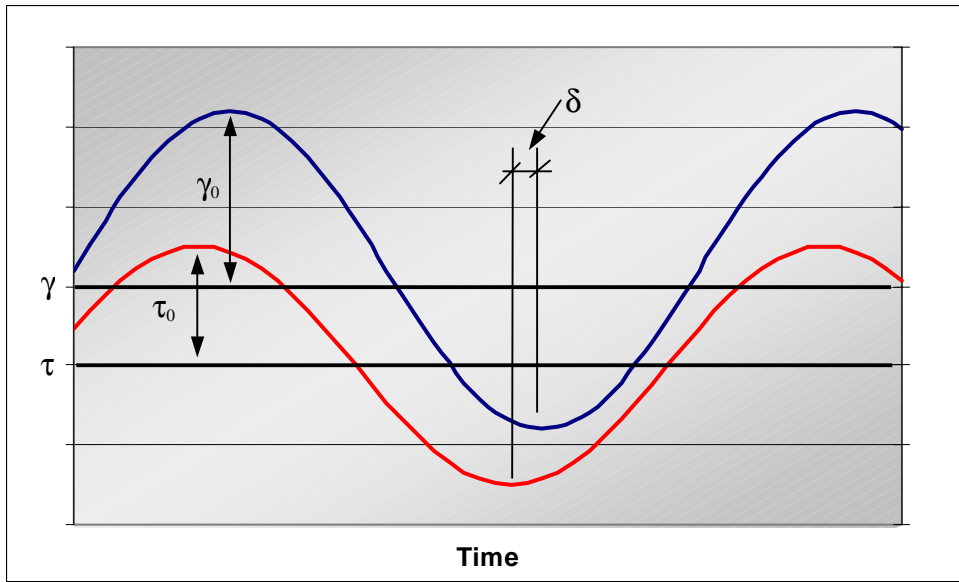
Figure 3.6: Dynamic experiment

$$\tau = \tau' + \tau'' = \tau'_0 \sin \omega t + \tau''_0 \cos \omega t \qquad \text{Eq. 3.17}$$

The two stress waves have the same frequency but different amplitude and a 90° phase angle in between (Figure 3.7) (Riande et al. 2000). The t' wave is in phase with the strain wave.
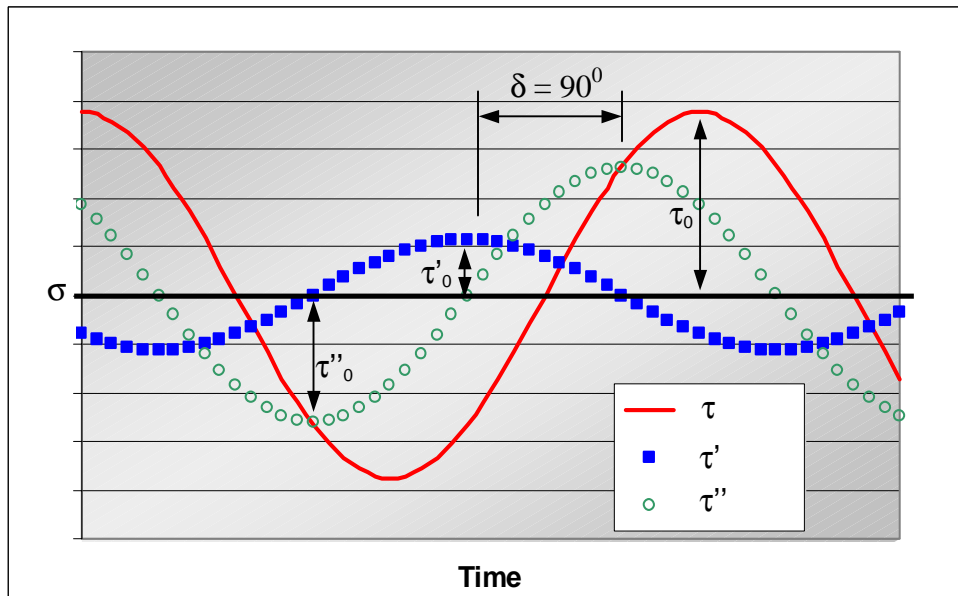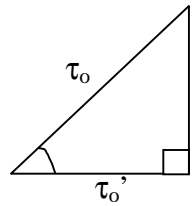
Figure 3.7: Stress wave decomposition

Since phase angle between the two waves is 90°, the phase angle can be defined as:
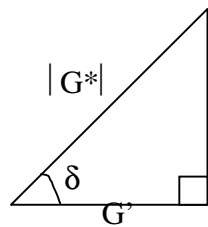
$$\tan \delta = \frac{\tau''_{o}}{\tau'_{o}} \qquad \text{Eq. 3.18}$$

From this, the elastic modulus can also be separated in two equations: the in phase or elastic modulus (G') and the out-of-phase, viscous or loss modulus (G''). These equations are:

$$G' = \frac{\tau'_{o}}{\gamma} \quad and \quad G'' = \frac{\tau''_{o}}{\gamma} \qquad \text{Eq. 3.19}$$

Equation 3.18 can now become:

$$\tan \delta = \frac{G''}{G'} \qquad \text{Eq. 3.20}$$

From geometry, it can be stated that:

$$\left| G^{*} \right| = \sqrt{\left(G'^{2} + G''^{2} \right)} \qquad \text{Eq. 3.21}$$

where:

$\left| G^{*} \right|$ = magnitude of the complex modulus (Pa)

The oscillation can also be written in terms of sinusoidal strain rate. The strain rate is:

$$\dot{\gamma} = \frac{d\gamma}{dt} = \gamma_0 \omega \cos \omega t = \dot{\gamma}_o \cos \omega t \qquad \text{Eq. 3.22}$$

In equation 3.22, a cosine is used since the strain rate is maximal when the strain is equal to zero and the strain rate is minimal when the strain is maximal. From this observation, it can be said that the strain rate wave is in phase with the out-of-phase stress wave (σ'').

From equation 3.22, it is clear that $\gamma_0 \omega = \dot{\gamma}_o$. Now, the strain rate can be substituted in equation 3.19 to obtain:

$$\frac{G''}{\omega} = \frac{\tau''_0}{\dot{\gamma}} \quad \Rightarrow \quad \tau''_0 = \frac{G'' \dot{\gamma}}{\omega} \qquad \text{Eq. 3.23}$$

and

$$\frac{G'}{\omega} = \frac{\tau'_0}{\dot{\gamma}} \quad \Rightarrow \quad \tau'_0 = \frac{G' \dot{\gamma}}{\omega} \qquad \text{Eq. 3.24}$$

Now consider a small change in stress due to a small change in strain:

$$d\tau = G d\gamma \qquad \text{Eq. 3.25}$$

This equation can also be written as:

$$d\tau = G \frac{d\gamma}{dt} dt = G \dot{\gamma} dt \qquad \text{Eq. 3.26}$$

The integral of equation 3.26 is:

$$\int d\tau = \tau = \int_{-\infty}^{t} G \dot{\gamma} dt = \int_{-\infty}^{t} G(t - t') \dot{\gamma} t' dt' \qquad \text{Eq. 3.27}$$

Where:

t' = variable from -∞ to the present time **t**; so **t-t'** equals zero

The strain rate from equation 3.22 is substitute in equation 3.27 to obtain:

$$\tau = \int_{-\infty}^{t} G(t-t')\dot{\gamma}_o \cos \omega t' dt' = \int_{0}^{\infty} G(s)\cos \omega(t-s)ds \qquad \text{Eq. 3.28}$$

where:

s = t-t'

By using the trigonometric relation that relates cosine and sin:

$$\tau = \dot{\gamma}_0 \int_{0}^{\infty} G(s)\cos \omega s\, ds \,\cos \omega t + \dot{\gamma}_0 \int_{0}^{\infty} G(s)\sin \omega s\, ds \,\sin \omega t \qquad \text{Eq. 3.29}$$

Equation 3.29 can be separated in two different waves like in equation 3.17 to obtain:

$$\sigma'_0 = \dot{\varepsilon}_0 \int_{0}^{\infty} E(s)\sin \omega s\, ds \qquad \text{Eq. 3.30}$$

$$\sigma''_0 = \dot{\varepsilon}_0 \int_{0}^{\infty} E(s)\cos \omega s\, ds \qquad \text{Eq. 3.31}$$

With equations 3.23 and 3.24 substituted in equations 3.30 and 3.31:

$$\tau'_0 = \frac{G'\dot{\gamma}}{\omega} = \dot{\gamma}_0 \int_{0}^{\infty} G(s)\sin \omega s\, ds \qquad \text{and} \qquad \tau''_0 = \frac{G''\dot{\gamma}}{\omega} = \dot{\gamma}_0 \int_{0}^{\infty} G(s)\cos \omega s\, ds$$

$$G' = \dot{\gamma}_0 \,\omega \int_{0}^{\infty} G(s)\sin \omega s\, ds \qquad \text{Eq. 3.32}$$

$$G'' = \dot{\gamma}_0 \,\omega \int_{0}^{\infty} G(s)\cos \omega s\, ds \qquad \text{Eq. 3.33}$$

Now, if **G** is transformed with equation 3.12, equations 3.32 and 3.33 become:

$$G' = \dot{\gamma}_0 \, \omega \int_0^\infty G_0 e^{-s/\lambda} \sin \omega s \, ds \qquad \text{Eq. 3.34}$$

$$G'' = \dot{\gamma}_0 \, \omega \int_0^\infty E_0 e^{-s/\lambda} \cos \omega s \, ds \qquad \text{Eq. 3.35}$$

Finally, solving for the two integrals before using equation 3.13:

$$G' = \frac{G_0 \omega^2 \lambda^2}{1 + \omega^2 \lambda^2} \qquad \text{Eq. 3.36}$$

$$G'' = \frac{G_0 \omega \lambda}{1 + \omega^2 \lambda^2} \qquad \text{Eq. 3.37}$$

so

$$G' = \sum_{k=1}^{k=n} G_k \frac{\omega^2 \lambda^2}{1 + \omega^2 \lambda^2} \qquad \text{Eq. 3.38}$$

and

$$G'' = \sum_{k=1}^{k=n} G_k \frac{\omega \lambda}{1 + \omega^2 \lambda^2} \qquad \text{Eq. 3.39}$$

As with the relaxation portion, equations 3.38 and 3.39 can be transformed to use the elastic modulus instead of the shear modulus, in which case Equations 3.38 and 3.39 become:

$$E' = \sum_{k=1}^{k=n} E_k \frac{\omega^2 \lambda^2}{1 + \omega^2 \lambda^2} \qquad \text{Eq. 3.40}$$

$$E'' = \sum_{k=1}^{k=n} E_k \frac{\omega \lambda}{1 + \omega^2 \lambda^2} \qquad \text{Eq. 3.41}$$

3.3 Construction of master curves

It is often practical to reduce all the data from the same test at different temperature to a reference temperature. By building a master curve, one can see the behavior of the material over a wide range of time or frequencies.

The Williams, Landell and Ferry (WLF) superposition principle (Williams et al., 1955) is one of the most popular principles relating the shift factor to the temperature (Findley et al., 1989). The WLF was successfully used to construct master curves for rheological response of asphalt binders (Anderson et al., 1994). Once the reference temperature is selected, the different frequency sweep curves collected at different temperatures can be shifted horizontally by a shift factor:

$$Log\ a_t = \frac{-C_1(T-T_o)}{C_2+(T-T_o)}$$

Eq. 3.42

where:

a_t = the shift factor

C_1 and C_2 = material constants

T = temperature of curve to be shifted

T_o = reference temperature

Figure 3.8 shows an example of master curve constructed from individual frequency tests done at different temperatures.

3.4 Summary

Dynamic modulus can be mathematically converted to stress relaxation modulus by using a modified Maxwell model. In stress relaxation, the relaxation time and the initial
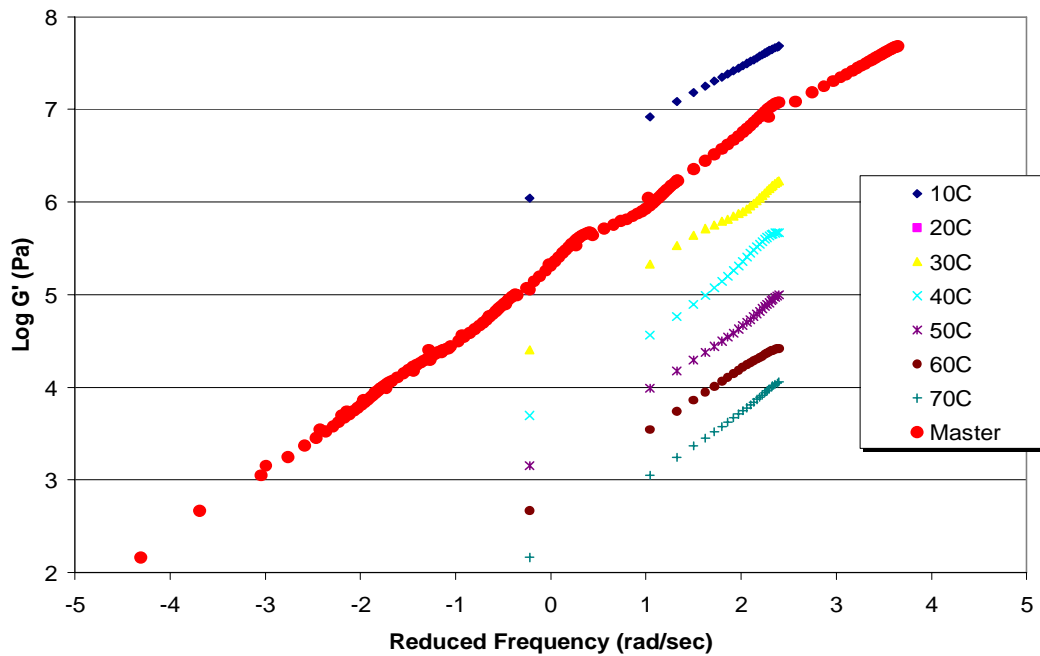
Figure 3.8: Example of master curve built from response curves at different temperatures.

modulus are the two variables that are needed in order to apply the models. Five sets of relaxation time and initial modulus are enough to model the complete relaxation curves. The relaxation time is the variable that links the dynamic modulus with the stress relaxation modulus.

CHAPTER 4 - MATERIALS AND METHODOLOGY

4.0 INTRODUCTION

This chapter describes the materials and test methods used in this research program. The material portion is separated in three sections: binder, aggregates and HMA mixtures. Binder and HMA tests are described in the methodology section.

4.1 Materials

Two different binders, three different aggregates types and two RAP sources were used in this research. This section describes those materials.

4.1.1 Binders

In order to evaluate the effect of the addition of RAP to HMA mix binder properties, two different PG virgin binders were chosen: 1) PG76-22, a polymer modified binder (SBS), and 2) PG64-22, an unmodified binder. These two binders are commonly used binders in Alabama. Table 4.1 shows the standard PG binder specification properties for both of these asphalt binders.

Figure 4.1 shows master curves for both of these binders using 22°C as a reference temperature. Note that there is little difference in the binder modulus at the colder temperatures (i.e., higher frequencies). Only at the warmer temperatures is there any appreciable difference in the modulus. Given these data, little difference is expected in the mix modulus when tested at 22°C or colder.

TABLE 4.1

Binder properties

Properties		PG 64-22	PG 76-22	Recovered Minnesota RAP Binder	Recovered Alabama RAP Binder
G* / sin δ, kPa (RTFOT)	64°C	4.228	-	-	-
	76°C	-	3.558	-	-
	88°C	-	-	4.65	2.613
Bending Beam Stiffness, S, MPa	0°C	-	-	101	-
	-12°C	179	127	-	169
Bending Beam Slope, m	0°C	-	-	0.315	-
	-6°C	-	-	-	0.348
	-12°C	0.323	0.363	-	-
	PG Grading	PG 64-22	PG 76-22	PG 88-10	PG 88-16

RTFOT = rolling thin film oven test
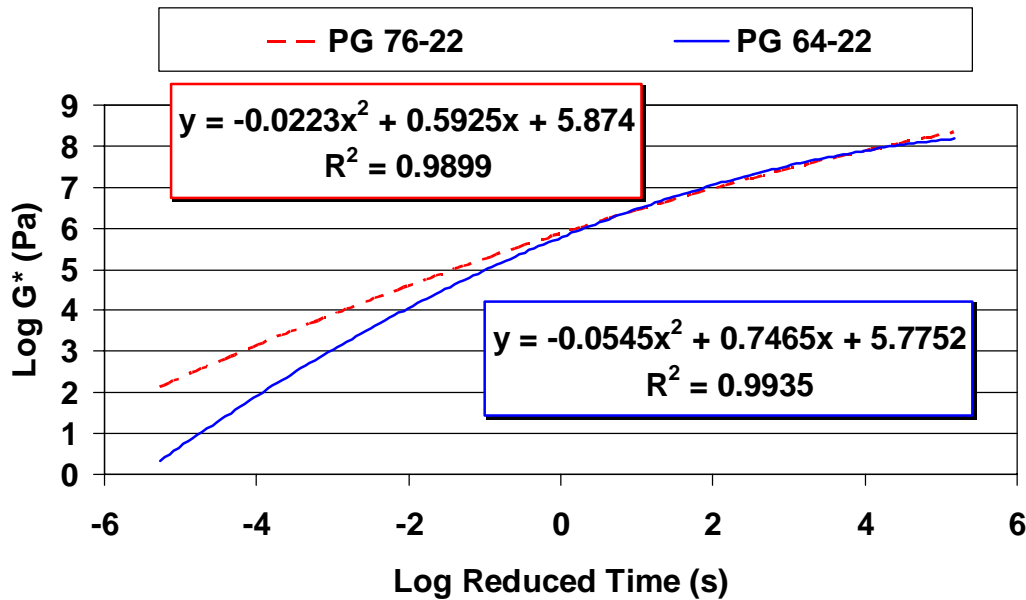
Figure 4.1: Binder G* master-curves at a 22°C reference temperature.

Within the figure:

PG 76-22   PG 64-22

$y = -0.0223x^2 + 0.5925x + 5.874$
$R^2 = 0.9899$

$y = -0.0545x^2 + 0.7465x + 5.7752$
$R^2 = 0.9935$

Y-axis: Log G* (Pa)
X-axis: Log Reduced Time (s)

4.1.2 Aggregates

Two sources of aggregates, a granite and a partially crushed river gravel, were selected to provide a range of aggregate shape and water absorption characteristics. Since selective absorption and adsorption of the asphalt binder or its components is possible, it was

considered desirable to also use a "model" aggregate that could be expected to have very low absorption and consistent, if any, adsorption at the asphalt-aggregate interface (Curtis et al., 1993).

Initially, glass beads of various sizes were considered for the model aggregate, assuming that the glass surface should not absorb any (or very little) of the binder. It was also assumed that the glass beads, being siliceous in nature, would be a good consistent representation of common aggregate mineralogy. However, the spherical shape of the beads is not representative of aggregate shapes used in HMA construction. Therefore, crushed and graded recycled glass was selected as the "model" aggregate.

All of the aggregate properties are shown in Table 4.2. Each of these aggregate stockpiles (natural and model) were sieved into individual fractions, and recombined to produce one of two gradations (Table 4.3).

TABLE 4.2

Aggregate properties

Properties	Granite	Gravel	Model Aggregate (recycled glass)	MN RAP*	AL RAP*
Bulk specific gravity	2.658	2.598	2.413	2.126	2.340
Bulk specific gravity, SSD	2.676	2.618	2.423	2.161	2.428
Apparent specific gravity	2.707	2.652	2.435	2.204	2.470
Water absorption, %	0.7	1.2	0.0	1.7	1.2
% Crushed Faces	100%	100%	100%	100%	100%
Flat and elongated, % (5:1)	0%	0%	100%	0%	0%
% Asphalt Binder	NA	NA	NA	5.6%	4.3%

NA = not applicable

* Values obtained on the RAP aggregate after solvent extraction.

TABLE 4.3

Gradations of materials used in this study

Gradation	Cumulative Percent Passing, %					
Sieve Size	Coarse Gradation	Coarse 50% AL RAP	Coarse 50% MN RAP	Fine Gradation	MN RAP	AL RAP
19.0 mm	100	100	100	100	100	100
12.5 mm	95	92	98	95	97	84
9.5 mm	85	82	92	85	92	76
4.75 mm	50	48	60	69	79	50
2.36 mm	31	31	40	55	66	32
1.18 mm	20	20	28	40	51	25
0.60 mm	15	15	19	30	33	19
0.30 mm	11	11	10	20	15	14
0.150mm	9	8	6	9	7	9
0.075 mm	5	5	4	5	4	6

4.1.3 Reclaimed Asphalt Pavement (RAP)

Two different sources of RAP were used in order to evaluate the sensitivity of the indirect tensile stress relaxation test method to a range of RAP properties. Alabama RAP was selected to represent RAP obtained from a region of the country that typically uses a PG 64-22. The Minnesota RAP was selected to represent region of the country that uses a softer grade of binder (e.g., PG 58-22). Both RAP sources were used at each of three concentrations of RAP: 15, 25 and 50%. Mixtures without RAP were used as the control mixtures (i.e., 0% RAP).

Table 4.1 shows binder properties for RAP binders extracted by ASTM D2172 (centrifuge) and recovered with a Rotavapor distillation process. Table 4.2 presents the aggregates properties of the RAP and Table 4.3 presents the after-extraction gradations for both sources.

The Alabama RAP source was visually more variable in it's content than the Minnesota RAP source. In order to minimize the heterogeneity of the RAP, three bags of RAP were mixed together before the amount of RAP used to prepare samples was obtained.

4.1.4 HMA mixes

The Brookfield concentric cylinder viscometer was used to evaluate the viscosity of the two binders over a range of temperatures so that the mixing and compacting temperature could be determined. According to Roberts et al. (1996) the mixing temperature is the temperature which gives a viscosity of 170 cPoise and the compacting temperature is the one that gives the binder a viscosity of 280 cPoise. For the PG64-22 (unmodified), the mixing and compacting temperature are respectively 150°C and 105°C.

This method of determining the mixing and compaction temperatures could not be used for the PG76-22 because it is a polymer-modified asphalt binder. Modified binders have higher shear rate-dependent viscosities, which results in artificially high temperature estimates of mixing and compaction temperatures (Azari et al., 2003). At the higher temperatures, some modified binders can start to degrade and change in composition (Shenoy 2001). In these cases, mix and compaction temperatures are typically estimated as 10°C higher than needed for an unmodified binder (Yildirim et al., 2000). Many authors have proposed different methods for estimating mixing and compacting temperature based on different shear rates; these are usually different than those used in the laboratory preparation of compacted samples. (Shenoy 2001, Yildirim et al., 2000, Azari 2003). Another author has proposed the mixing temperature can be increased

higher than 163°C as long as the binder does not start to emit smoke (Stuart 2002). In that study, they also proposed the use of a viscosity level of 1100 cPoise to find the compacting temperature for all binders with PG64-XX and above. For this research project a mixing temperature of 163°C and a compacting temperature of 120°C were used for the PG 76-22.

Conventional compacted HMA samples were prepares with a Superpave gyratory compactor following the ASTM D4013 standard using 100 gyrations. All specimens had a diameter of 150 mm and a height of around 115mm which results in air voids of around 4%. Pure (100 %) RAP samples were also prepared. This was done by heating the RAP at 160°C for four hours, then compacted with 100 gyrations of the SGC compactor. Table 4.4 shows all the conventional HMA samples with and without RAP that were compacted. Three replicates were fabricated for each HMA mixture.

The HMA mixtures with the model aggregates were compacted with a manual Marshall hammer to avoid breaking the glass particles during compaction; these samples had air voids of around 3%.

4.2 Test Method Descriptions

A parallel plate DSR was used to determine both the dynamic and relaxation modulus of both the virgin binders used in this study. The shear complex modulus and shear stress relaxation modulus values were calculated from this testing.

4.2.1 Dynamic Modulus of Binders

A TA Instruments AR1000 constant stress parallel plate DSR was used for the dynamic experiment. A frequency sweep covering a range of 0.6 to 250 rad/s on samples with

both 8 or 25mm in diameter was used to establish the minimum and the maximum frequencies that could be used with this DSR. In order to be able to build master curves for the dynamic modulus of the binders, testing was completed for a range of temperatures (5, 10, 22.5, 30, 40, 50, 60, 70 and 80°C).

Table 4.4 Average air voids content for the mixes

Asphalt	Type of RAP	% of RAP	Average Air Void (%)			
			Granite		Gravel	
			Fine Grad.	Coarse Grad.	Fine Grad.	Coarse Grad.
PG 64-22		None	4.5	3.8	5.0	4.6
	AL RAP	15%	3.4	3.5	5.8	5.0
		25%	3.7	4.2	5.4	3.8
		50%	3.4	4.0	3.4	4.5
	MN RAP	15%	3.1	2.5	5.6	5.5
		25%	3.5	3.0	2.8	2.8
		50%	2.0	2.8	2.5	2.2
PG 76-22		None	4.1	3.6	4.5	3.7
	AL RAP	15%	2.9	2.7	5.2	4.7
		25%	3.7	4.4	4.2	4.2
		50%	2.4	3.2	5.6	3.2
	MN RAP	15%	3.5	2.3	4.9	5.0
		25%	3.3	3.0	4.1	4.2
		50%	1.6	3.3	3.8	2.7
AL RAP		100%	3.0			
MN RAP		100%	2.9			

For the purpose of this research, the upper temperature was selected to encompass the highest PG temperature (i.e., 76°C for the PG 76-22). The lowest temperature (5°C), while -22°C was ideal, was the coldest practical temperature that could be used with this equipment. Three samples of the same binder were tested at each temperature. The first test was done at 5°C and once completed, the temperature was increased to the next warmer test temperature in the sequence. To ensure that the temperature was homogeneous throughout the sample, the sample was held at the test temperature for 10

minutes after the test temperature in the environmental chamber was reached and stabilized (ASTM P246). This procedure was followed for each incremental increase in test temperature.

One of the assumptions in DSR testing is that the binder modulus is constant in the linear viscoelastic region. This assumption was verified prior to any dynamic modulus testing by conducting tests at different strain level and different frequencies, then comparing the resulting modulus. When the modulus starts to change, the linearity limit is reached. In order to fix the linearity limit, a threshold value needs to be set. In this case, when the modulus changed of more than 10%, the limit was considered reached (ISAP 2005) (Figure 4.2).
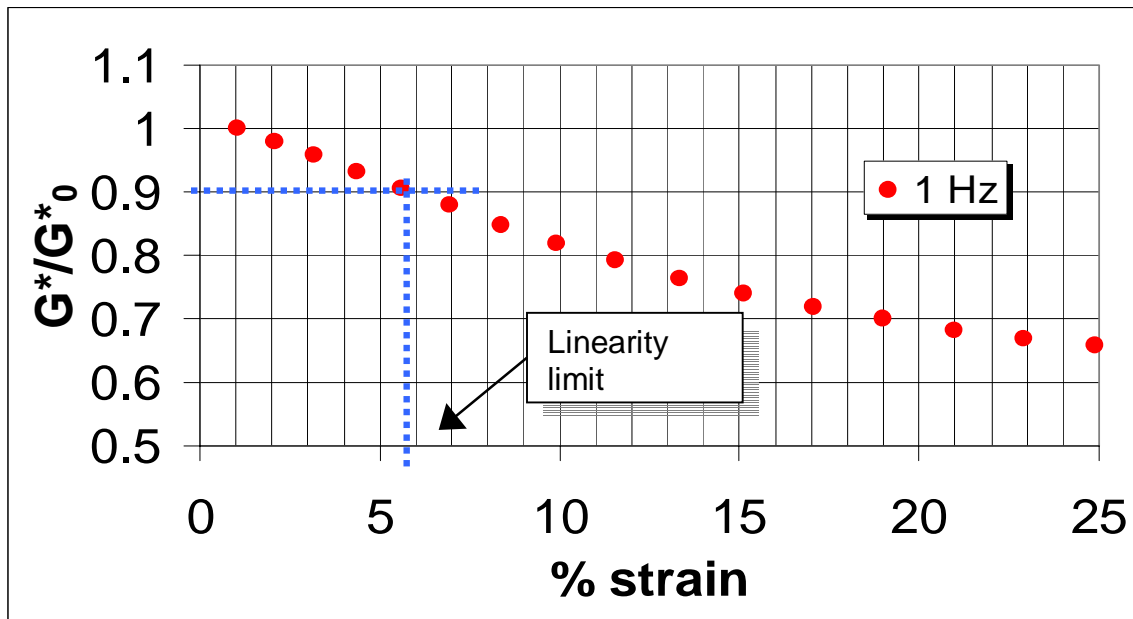
Figure 4.2: Example of linearity limit (PG 64-22 at 30°C)

At the lower temperatures (5 and 10°C) the strain was controlled by the capacity of the DSR and not the linearity limit. At low temperature and high frequencies (above

60 rad/s) the binder is so stiff that the DSR does not have enough torque to provide the desired strain. For example, the strain limit at 5°C is 0.35% because that is the maximum strain that the DSR can achieve at 250 rad/s. It should be noted that the sample geometry was also chosen as a function of the temperature. For temperature below 40°C, the sample had an 8 mm diameter and a thickness of 2 mm. At higher temperature, the samples had a larger diameter of 25 mm in diameter and a thickness of 1 mm. The different strain levels used in this testing program are shown in Table 4.5. The same limits were used for both binders. Since higher strain will result in higher stress, the maximum limits shown in this table were used. By using higher strains, there is less error in the results since the amplitude of both the strain and stress are much bigger than the sensor noise range in the apparatus.

Table 4.5: Strain used in the dynamic modulus test for both binders (DSR AR 1000)

Temperature (^{o}C)	Strain (%)
5	0.35
10	0.5
20	1
30	5
40	10
50	10
60	10
70	15
80	15

4.2.2 Stress Relaxation of Binders

The binder stress relaxation test was conducted with a parallel plate DSR. This test was used to evaluate stress relaxation characteristics of virgin asphalt binders. A TA

Instruments AR2000 was used to conduct 8 and 25mm diameter parallel plate stress relaxation testing at five different temperatures (5, 22, 30, 40 and 50°C). It should be noted that different DSR equipment were used for the dynamic and stress relaxation tests. While the DSR for dynamic modulus was available through the NCAT laboratory, arrangements had to be made for the temporary loan of a research-grade DSR unit capable of stress relaxation testing with TA Instruments.

As with the dynamic modulus testing, all stress relaxation tests were performed within the linear viscoelastic (LVE) range of the behavior of the binder. To find the limit of the LVE range, relaxation tests were performed at different levels of constant strain. The same threshold, a decrease of more than 10%, was used to set the LVE limit. Table 4.6 shows the strain levels used as a function of the temperature.

TABLE 4.6
Strain level as a function of the temperature for both binders tested
(parallel plate configuration)

Temperature (^{o}C)	Strain (%)
5	0.1
10	0.5
22	2.0
30	5.0
40	5.0
50	6.0

Another important point that needs to be considered in relaxation test is the time needed to reach a constant strain level. As noted in Chapter 2 - Literature Review, one of the main reasons for other researchers not using stress relaxation testing is the inability to quickly achieve the desired, and stable, strain level. Ideally, the relaxation modulus should only be calculated from the moment at which the constant strain is achieved (Chen

2000). With the DSR used in this experiment, it took between 0.1 and 0.35 seconds to reach the desired strain; the length of time varies depending on the testing temperature (Figure 4.3). Since consistency along the time axis was needed for comparing the results from different temperatures, a time of 0.35 seconds was selected as the starting point for the calculation of the stress relaxation modulus for the binder testing.
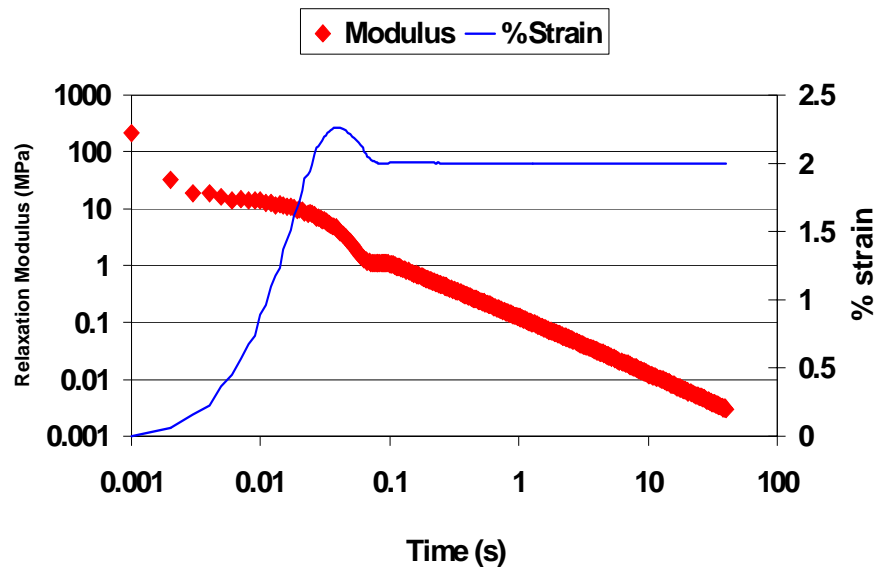
Figure 4.3: Example of time needed to reach constant strain
for binder relaxation test (PG 64-22 at 22°C)

The strain was maintained for a maximum of two minutes because preliminary testing indicated that the stress relaxation was substantially achieved within that time, regardless of temperature. Measurable loads were not usually obtainable at test times longer than 2 minutes. By default, the DSR acquires a thousand points of data per second. This amount of data was found to be sufficient to define the material behavior.

Three samples of both binders (PG 76-22 and PG 64-22) were tested at each of the same temperatures used for dynamic modulus testing. The average result for each temperature was then used for analysis.

4.2.3 HMA IDT Stress Relaxation Test

An Instron 8501 was used to conduct the IDT stress relaxation test on compacted HMA samples. The strain was set using the ram control displacement sensor, and a 22KN load cell was used to measure stress relaxation every 0.1 seconds over a time interval of up to two minutes. Eventually, the test time was limited to 45 seconds because only minimally measurable decreasing changes in stress, regardless of temperature, were obtained after this time.

Originally, the jig for indirect tensile strength testing when evaluating the moisture sensitivity of HMA mixtures (ASTM D4867) was used to hold the sample. The posts appeared to generate some friction so the first modification to the test equipment was to refit the load frame so that the upper and lower platens were vertically aligned but not mounted on guide posts.

The test method development included:

- Defining of a range of strain levels within the linear viscoelastic range,

- Evaluation of the time needed to achieve a constant strain, evaluation of the time needed for data collection, and

- Development of an analysis approach for estimating initial modulus and the rate of stress relaxation.

Testing parameters were evaluated at two test temperatures: 5 and 22°C.

4.2.3.1 Test Method Development

Like for the binder experiment, it was necessary to establish the limit of the linear viscoelastic range for the different HMA mixtures when tested at different test

54

temperatures. Tests were performed at different strain levels and the relaxation modulus was calculated. The LVE limit was considered attained when the relaxation modulus has decreased 10% compared to the modulus measured at the lowest strain level. At 22°C, the average strain level was 0.0013 with a coefficient of variation of 20%. At 5°C, the strain level was 0.0006 with a coefficient of variation of 30%.

The ramp speed was found to have a large influence on the precision of the level of strain achieved. The faster the ram moves, the less control there is on the level of strain. Since in a relaxation experiment it is desirable to reach a known constant strain as fast as possible without over-shooting the target strain, a ram speed of 100 mm/min was chosen.

The time to constant level of strain was also analyzed. The Instron software used to gather the data was set to only start acquiring data when the strain was constant, so the change in stress before this point could not be considered in the analysis. To ensure that the stress relaxation analyzed comes from the sample tested and not the equipment setup, an elastic (steel) cylinder was tested. Steel, under the low level of stress used in this experiment, is not supposed to show any relaxation; so if there is relaxation, it can be attributed to one or more equipment components. Figure 4.4 shows that it takes less than 3 seconds to reach a modulus that is constant for the steel cylinder; a difference of 1% or less was considered to be acceptable.

4.3 Summary

For this research project, different materials were used: 1) a PG 64-22, an unmodified asphalt binder, and 2) a PG 76-22 polymer modified asphalt binder. Both binders were
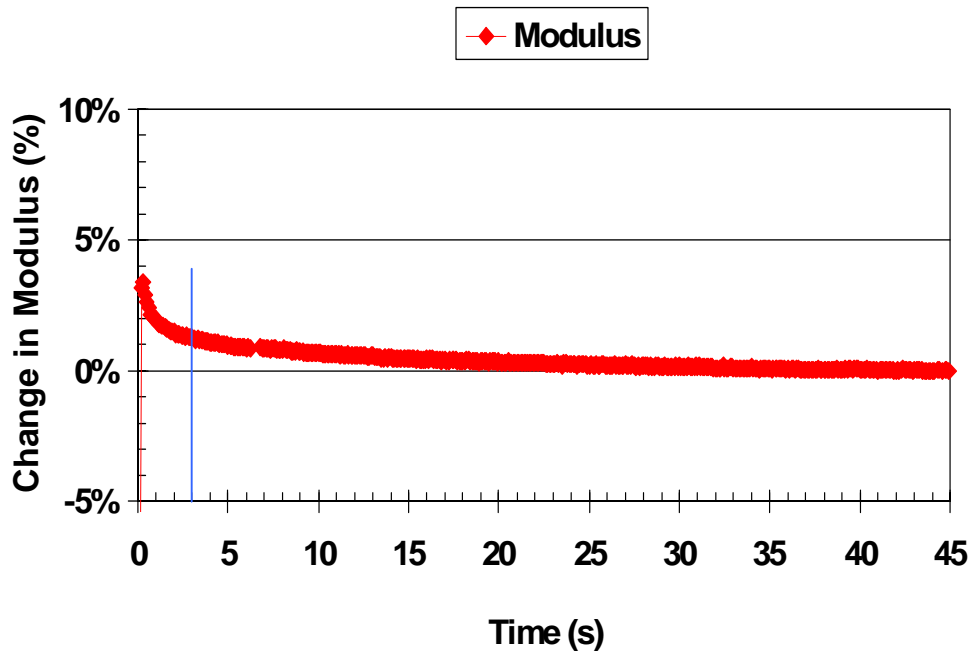
Figure 4.4: Setup time with steel cylinder in HMA IDT stress
relaxation equipment (22°C)

found to have similar master curves for temperatures at or below 22°C; above 22°C, the

difference in the stiffness and the relaxation capacities of the binders increases with

increasing temperature. Dynamic modulus and stress relaxation tests were performed on

both binders. For both tests, the controlled strain was kept in the limit of the linear

viscoelastic region of the behavior of the binders.

The dynamic modulus was determined for these binders using a frequency sweep

between 0.6 and 250 rad/sec at each of 9 different temperatures between 5 and 80°C.

Stress relaxation testing was conducted at only 6 different temperatures between 5 to

50°C were used due to equipment limitation.

HMA mixtures were prepared with one of three aggregate sources: 1) a model

aggregates simulated with crushed glass, 2) a 100% crushed granite, and 3) a

predominately crushed river gravel with a high absorption capacity.

CHAPTER 5 - RESULTS AND DISCUSSION

5.0 Introduction

This chapter presents the results and analyses, in the following order:

- Relation between the dynamic and the relaxation modulus for the binders.

- Comparison of the asphalt binder and HMA mixture stress relaxation results.

- Statistical analyses.

- Methodology for selecting either the percent of RAP or grade of virgin asphalt binder based only on testing compacted HMA samples.

5.1 Relationship Between Dynamic Modulus and Relaxation Modulus

   (Binders Only)

As described in Chapter 3 – Original Analysis Hypothesis, it is mathematically possible to use dynamic modulus results to obtain relaxation modulus. Figures 5.1 shows an example of the relation between the measured asphalt binder shear dynamic modulus and the stress relaxation predicted dynamic modulus. It shows that the relation between the measured and predicted moduli is linear, but it is not perfectly on the equality line (i.e., slope of 1.00). Possible reasons for this are:

- Equipment differences in the DSR devices that needed to be used for dynamic modulus testing (NCAT DSR) and the stress relaxation testing (TA DSR).

- The stress relaxation test results obtained with the TA AR2000 model may be slightly off because of the time needed to reach constant strain. The very early time results had to be discarded due to the strain levels not having reached a constant value quickly (see Figure 4.3). It is anticipated that higher moduli values would be those obtained from very short loading times.

- The time between the sample preparation and the test was longer for the relaxation tests than for the dynamic modulus tests which results in stiffer binder due to internal structuring of the molecules (Bell 1989).
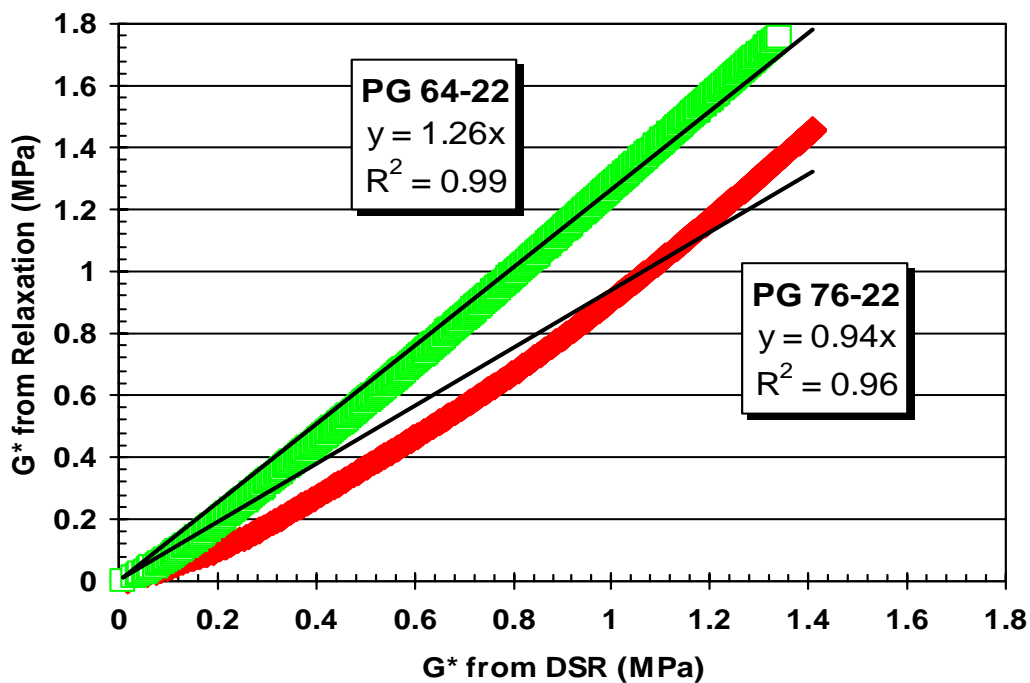
Figure 5.1: Relation between measured and calculated shear dynamic modulus for both binders at 22°C

Results are similar at both temperature. Modulus values range from about 0 to close to 30 MPa when binders are tested at 5°C; they only range from about 0 to less than 2 MPa at 22°C. The good correlation indicated by R^2 values of at least 0.96 indicate that

changes in the stress relaxation modulus for a given binder is a good representation of changes in the binder's dynamic modulus. However, the slope of the relation changes with each test (Figure 5.2). The fact that the slope change and that the coefficient of variation of the slope is high make the use of those relation complicated.
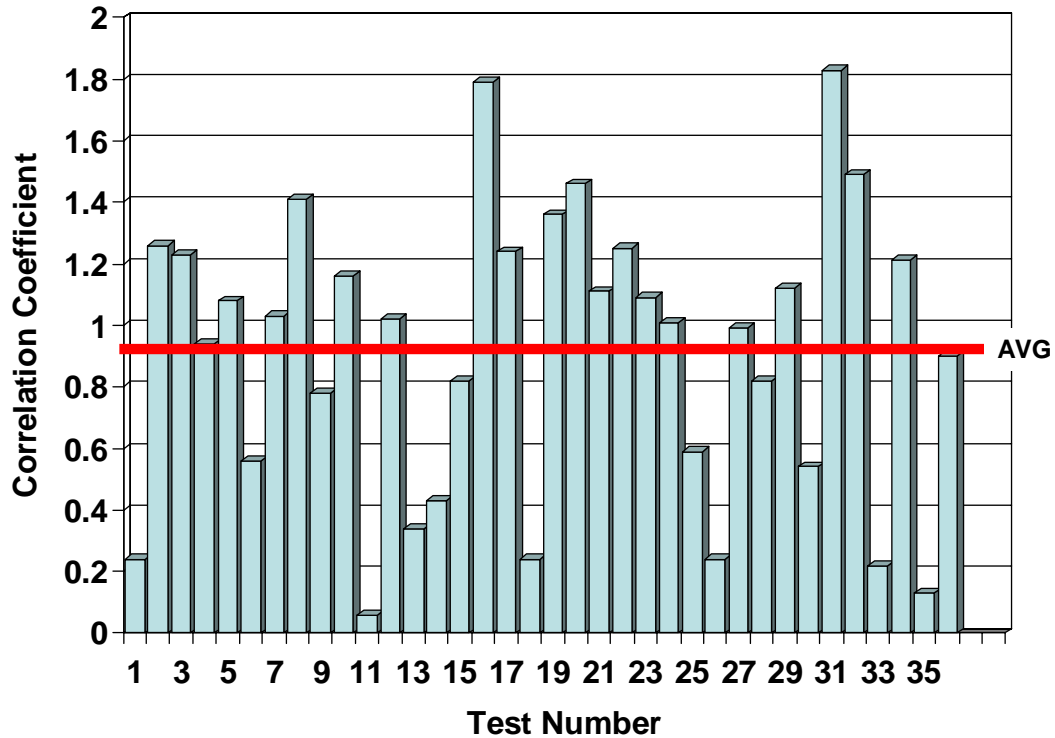
Figure 5.2: Relation between measured and calculated shear dynamic modulus

5.2 Comparison of Binder and HMA Stress Relaxation Test Results.

5.2.1 HMA Mixtures with Model Aggregates

It was hypothesized that the aggregate in the mix should have little to no effect on the indirect tension stress relaxation modulus of the HMA mixes since the asphalt binder is the only component that can provide tensile strength. The theoretical basis of this hypothesis was explored through the testing of HMA mixtures made with the model

aggregate. Figure 5.3 shows the relationship between the average stress relaxation modulus at 22°C of the PG 76-22 asphalt binder and the average HMA indirect tension stress relaxation modulus.
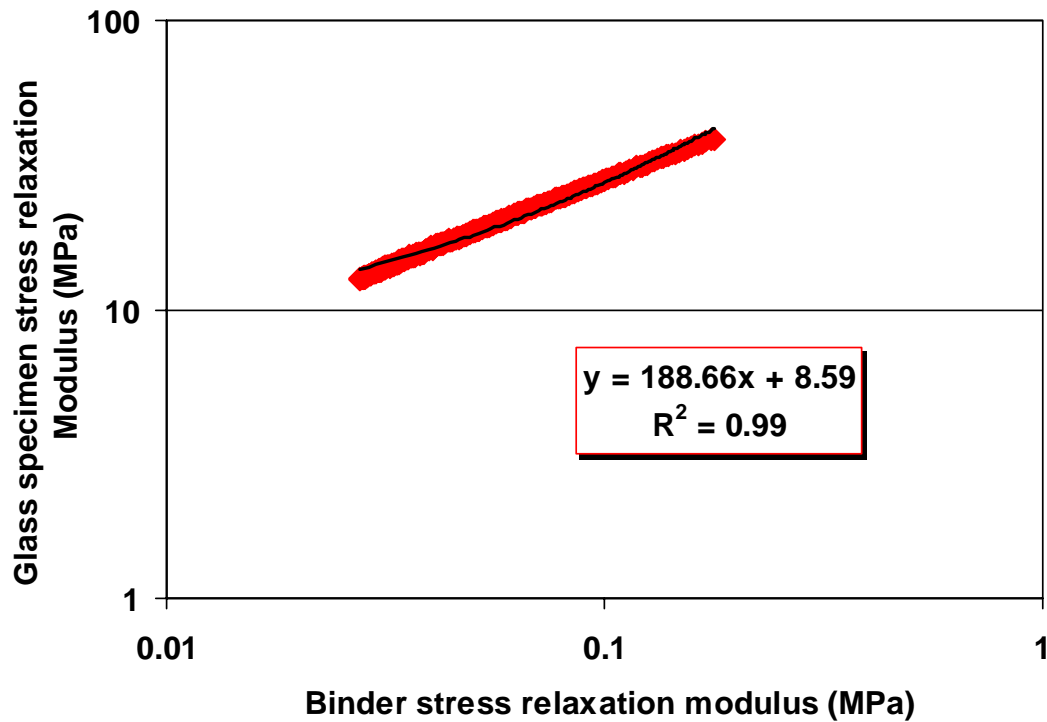
Figure 5.3: Relation between binder relaxation modulus (PG 76-22) and HMA indirect tension stress relaxation modulus (model aggregate) prepared with the same PG 76-22 and tested at 22°C

The strain for the model HMA stress relaxation modulus was calculated using an estimated horizontal strain. The vertical displacement of the ram was divided by the diameter of the sample to calculate the vertical strain. The horizontal strain was then estimated using an assumed Poisson's ratio, μ, which was selected base on the temperature (0.35 for 22°C and 0.2 for 5°C):

$$\varepsilon_h = \varepsilon_v \, \mu \hspace{4cm} \text{Eq. 5.1}$$

Where:

ε_h = horizontal strain

ε_v = vertical strain

μ = Poisson's ratio

It should be noted that linear stress relaxation modulus of the HMA, E, was converted to a shear relaxation modulus, G, by the following equation (Cook and Young 1999):

$$E = 3\,G \hspace{5cm} \text{Eq. 5.2}$$

Figure 5.3 shows that there is a good linear log-log relationship between both relaxation modulus, however there is a pronounced effect on the modulus with the inclusion of the solid particles in the binder film. That is, the model HMA stress relaxation modulus is consistently higher (stiffer) than the stress relaxation modulus of the virgin asphalt binder. This is expected since the inclusion of solid particles in any liquid increases the viscosity of the liquid, therefore the higher stiffness for the mixes is assumed to be a function of the percentage of fines that is incorporated into the combined binder-aggregate film (Buttlar et al., 1999). The stress relaxation modulus of the model HMA mix is about 10 MPa when the binder stress relaxation modulus is 0.01 MPa and 100 MPa when the binder stress relaxation modulus is 1 MPa. These results indicate that the stress relaxation modulus of the binder will be significantly increased by the presence of solid particles.

While the stress relaxation moduli magnitudes are different, the indirect tension stress relaxation testing of an HMA mixture can be expected to represent corresponding changes in the stress relaxation modulus of the asphalt binder.

5.2.2 HMA Mixtures with Standard Aggregate

The work with the model HMA mixtures showed that indirect tension stress relaxation test on HMA mixture is a good indicator of the binder properties. Work continued with the test method development using HMA mixtures with two gradations with each of two aggregate sources. Like for the model aggregate, the correlation coefficient of the relation between the binder relaxation modulus and the HMA relaxation modulus is very good ($r^2 > 0.9$), but the slope of the relation varies a lot. Figure 5.4 presents the average slope of the relation for the different mixes. It can be noted that the slope differs from one type of mix to another and that the coefficient of variation is high in all cases
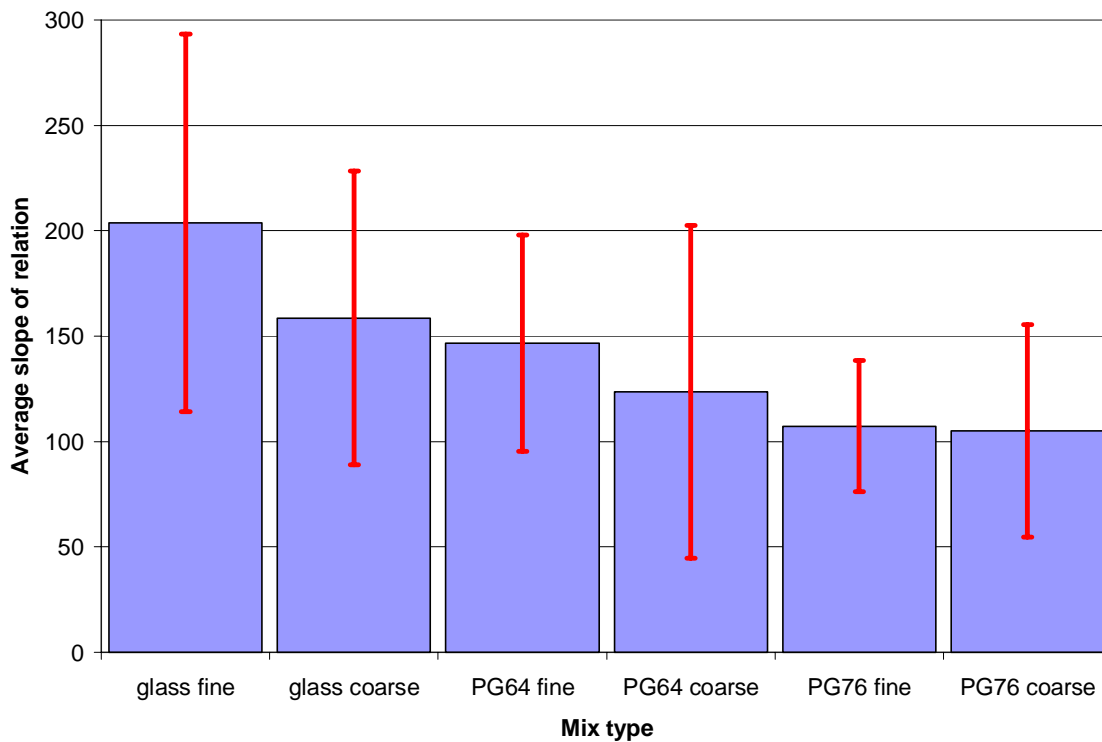
Figure 5.4: Average slope of the relation between binder relaxation modulus and HMA relaxation modulus

5.3 Statistical Analysis

A best fit curve approach was used to model the changes in indirect tension stress relaxation modulus with time (Figure 5.5). A power curve was, in every case, the best fit curve with an R^2 of 0.9 or above, regardless of the test temperature. The influence of when the data collection is started was investigated next.

On Figure 5.5, two curves for which the data collection was started at different times are shown. The resulting correlation equations have a difference of less than 1% in either the intercepts or exponents. These results indicate that while obtaining data at times closer to zero would provide more accurate zero-time information, there is a sufficient amount of stress relaxation information to estimate the mix characteristics using less than ideal testing conditions.
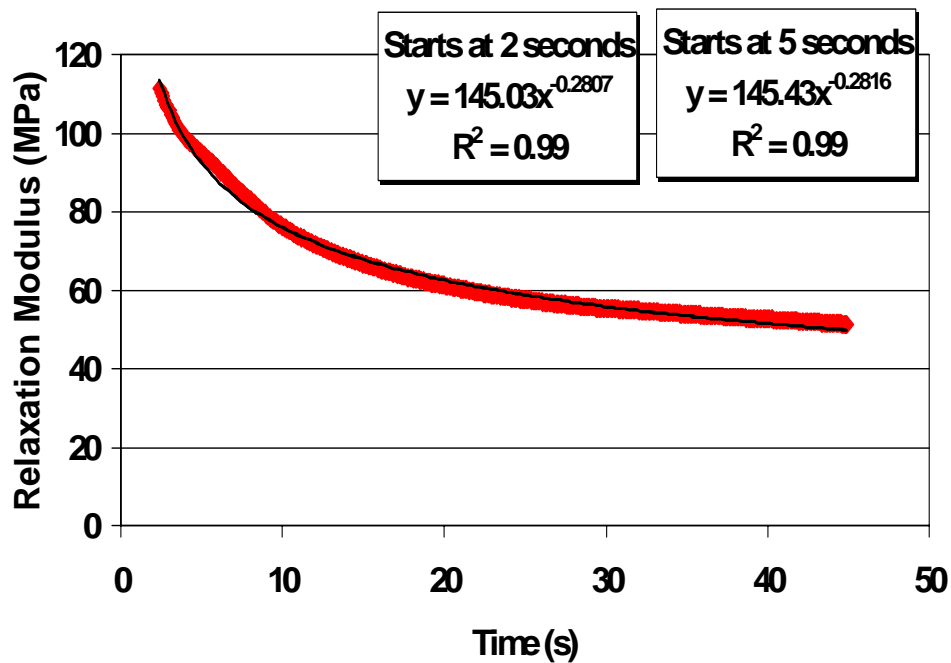
Figure 5.5: Typical relaxation curve and best fit curves.

There are two key parameters in the power model that can be used to evaluate changes in the mix properties due to changes in the asphalt binder properties. These are

the intercept and the exponent. The intercept represents the maximum modulus as time approaches zero. The exponent, which is function of the degree of curvature, represents the ability of the sample to relax. The exponent with be referred to hereafter as the curvature coefficient. The higher the value of the exponent, the more the HMA mixture relaxes in a given period of time. Statistical analyses were completed using these two parameters. The first statistical evaluation calculated the Pearson's correlation matrix to determine if there were any well-correlated single variable comparisons. This analysis showed there were only two fair correlations found for each of the two test temperatures:

- Modulus increased with the addition of RAP (R=0.59 at 5°C and 0.65 at 22°C).

- Curvature coefficient decreased with the addition of RAP (R=0.76 at 5°C and 0.66 at 22°C).

These correlations are as expected. That is, modulus should increase as more RAP binder is incorporated into the HMA effective binder. Also, as more RAP binder is included in the overall HMA binder properties, the ability of the mix to deform with time (i.e., relax) should be reduced. This is because asphalt binders lose their ductility as they age.

The next statistical evaluation used an analysis of variance (ANOVA) followed by the Duncan multiple range test (Cody and Smith 1997). With the Duncan analysis, it is possible to separate the data into groups that have significant difference in their means. The effect of PG grade, percentage of RAP, gradation, aggregate source, and RAP source on the stress relaxation modulus and the curvature coefficient were analyzed. The complete results used for the statistical analyses are shown in Appendix B.

5.3.1 Effect of Gradation, Aggregate Source and RAP Source

No statistical differences in either the modulus (intercept) or curvature coefficient (exponent) were found as the result of changes in the gradation, aggregate source, or RAP source. This is in agreement with the preliminary findings that showed minimal influence of the gradation. As for the aggregates sources, it was also expected since the IDT stress relaxation test is primarily an indicator of the binder properties. Finally, the RAP source did not make any statistical difference because there is little difference between the PG grades of both RAP binders. It should be noted that the high variability in the Alabama RAP, noted previously as visibly variable material, may have produced enough variability in the HMA mixture properties to hide any statistical difference that could have been seen otherwise (e.g. due to the RAP gradation).

5.3.2 Effect of Virgin PG Grade

For the analysis on the effect of the PG grade on the modulus and the curvature coefficient, only data from the HMA samples without RAP were used (Table 5.1). The Duncan multiple means test shows that neither the average initial stress relaxation modulus nor average curvature coefficient were significantly different at a given test temperature. However, the trends in both mix properties are consistent with expectations. The modulus increases with decreasing temperature, with little difference between the binders at the cold temperatures and a slight, but not statistically different, change at the warmer temperature. This agrees with the differences seen in the binder master curves (Figure 4.1 in Chapter 4).

The curvature coefficient is lower at the colder temperature, and dependent upon the binder grade at the warmer temperature. The curvature coefficient is less for the polymer modified PG 76-22 than for the PG 64-22 at 22^oC, indicating that the polymer modified asphalt will take longer to relax at the warmer temperature.

Table 5.1
Influence of the PG grade on the relaxation
modulus and the curvature coefficient (No RAP)

	Temp. (^oC)	Duncan Grouping	Mean	COV (%)	n	Binder Grade
Modulus (MPa)	5	A	220.6	24	24	PG 64-22
			206.6	34	24	PG 76-22
	22	A	112.7	33	24	PG 64-22
			103.3	34	24	PG 76-22
Curvature Coefficient	5	A	0.123	18	24	PG 64-22
			0.116	24	24	PG 76-22
	22	A	0.371	20	24	PG 64-22
		B	0.267	51	24	PG 76-22

5.3.3 Effect of the Percentage of RAP

For this analysis, the results from mixes with and without RAP were used (Table 5.2). At 5^oC, adding 15% of RAP at least doubles the initial stress relaxation modulus; no significant increases are seen with further increases in RAP. The curvature coefficient is more sensitive to the percentage of RAP as is seen by the continually decreasing ability of the HMA to dissipate stress over time with an increasing percentage of RAP. Both the control (no RAP) and 15% RAP mixtures have statistically similar curvature coefficients; at least 25% RAP is needed to produce a statistically significant decrease. The curvature coefficient is similar for both the 50 and 100% RAP mixtures, and both are significantly different from the control (no RAP).

Table 5.2
Influence of the percentage of RAP on the
relaxation modulus and the curvature coefficient

	Temp. (°C)	Duncan Grouping		%RAP	Mean	COV (%)	n
Modulus (MPa)	5		A	0	213.6	29	48
				15	507.9	29	48
			B	25	513.1	27	48
				50	517.1	34	48
				100	443.6	47	11
	22		A	0	108.0	34	48
			C	15	190.0	36	48
		B		25	204.9	35	48
			D	50	237.6	29	48
				100	258.8	18	11
Curvature coefficient	5		A	0	0.318	21	48
		B		15	0.281	32	48
				25	0.242	29	48
			C	50	0.148	46	48
				100	0.153	101	11
	22		A	0	0.119	38	48
		B		15	0.097	21	48
				25	0.082	16	48
			C	50	0.051	46	48
				100	0.057	41	11

At 22°C, the initial stress relaxation modulus doubled with the inclusion of any percent RAP in the mixes. There is a statistically significant increase in the modulus when using as little as 15% RAP at this temperature. There is no difference between mixes with either 15 or 25% RAP. Mixes with either 50 or 100 % RAP have similar modulus and both are significantly higher than mixes with lower percentages of RAP. The same trends are seen for the curvature coefficient at this temperature.

5.4 Evaluation of Current Blending Chart Practices for Estimating the Percent of RAP or Grade of Virgin Binder

The current practice for determining the percent of RAP to use in a new HMA mix uses blending charts, which assumes that there is a linear relation between the amount of RAP and the binder properties of the composite mix from 0 to 100% RAP. When mixtures with a range of RAP from 0 to 50% are considered, the assumption of linearity between modulus and the percent of RAP is valid. Figure 5.6 shows the relationship for mixes containing Minnesota RAP and PG 64-22 binder tested at 22°C; the other mixes, while not shown, have similar relationships.
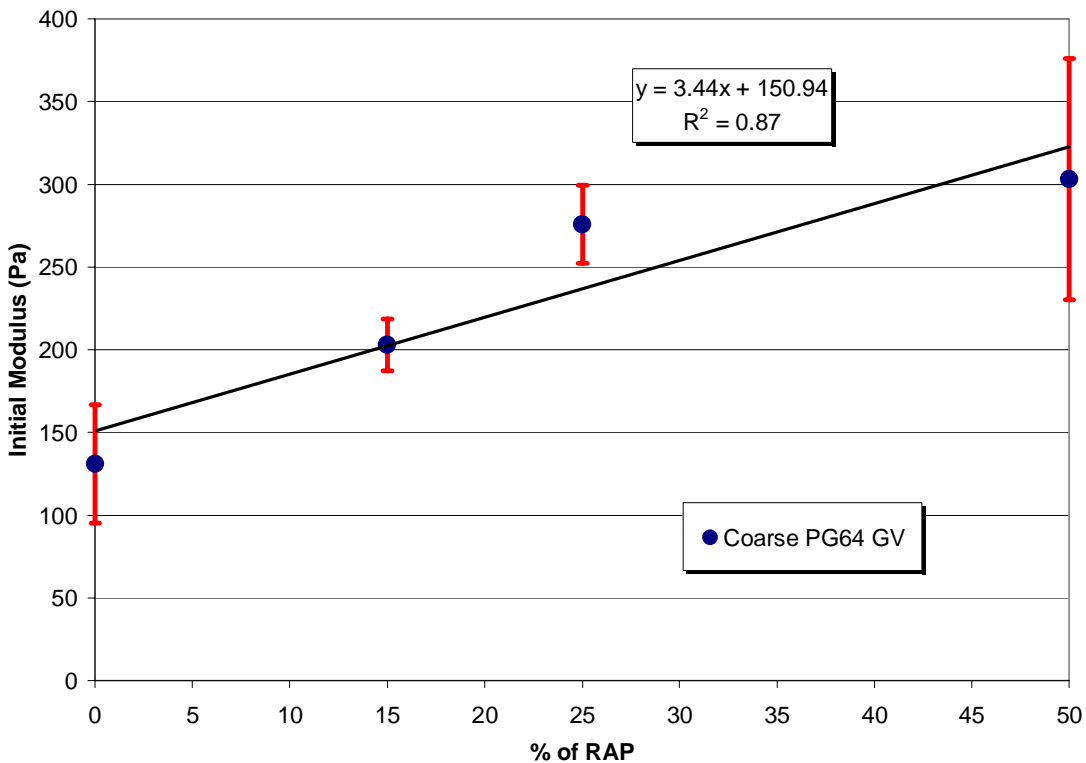
Figure 5.6: Linear relation between percent of RAP and
modulus (MN RAP, Gravel, PG 64-22, 22°C)

To represent the 100% recovered binder used for constructing the binder-only blending charts, 100% RAP samples were compacted and tested. As shown previously, there is no significant difference between samples with 50 and 100% RAP. Because of that, if the 100% RAP samples are added to the Figure 5.6, it is obvious that the relation is no longer linear (Figure 5.7).
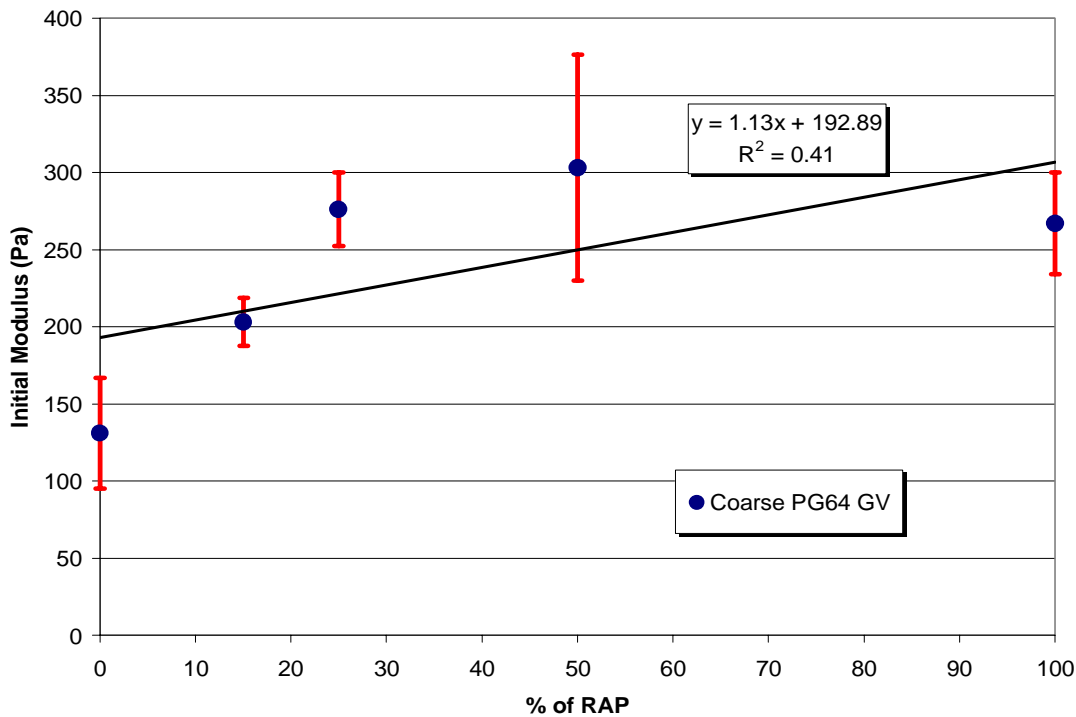
Figure 5.7: Relation between percent of RAP and
modulus (MN RAP, Gravel, PG 64-22, 22°C)

This figure shows that an assumption of a linear relationship between the limits of no RAP and 100% RAP are not supported when the HMA mix is evaluated; the relationship is in fact non-linear. These same trends were seen for all of the other binder-RAP mixes (not shown).

If the guidelines for blending RAP in a new mix are applied to the indirect tensile stress relaxation modulus results, an addition of 10, 15 and 25% of RAP would result in an increase of modulus of 5, 7.5 and 12.5% respectively, according to Figure 5.7. But

since the relation is really non-linear, the increase of modulus should more realistically be estimated as 15, 22.5 and 37.5%, respectively. These blending charts were constructed with the data presented in Tables 5.4a and 5.4b.

The curvature coefficient can also be used to create blending charts. Figures 5.8 and 5.9 show that, as for the stress relaxation modulus, there is a good linear relation between the curvature coefficient up to 50% of RAP but the relation is not as linear if the blending chart includes 100% RAP.
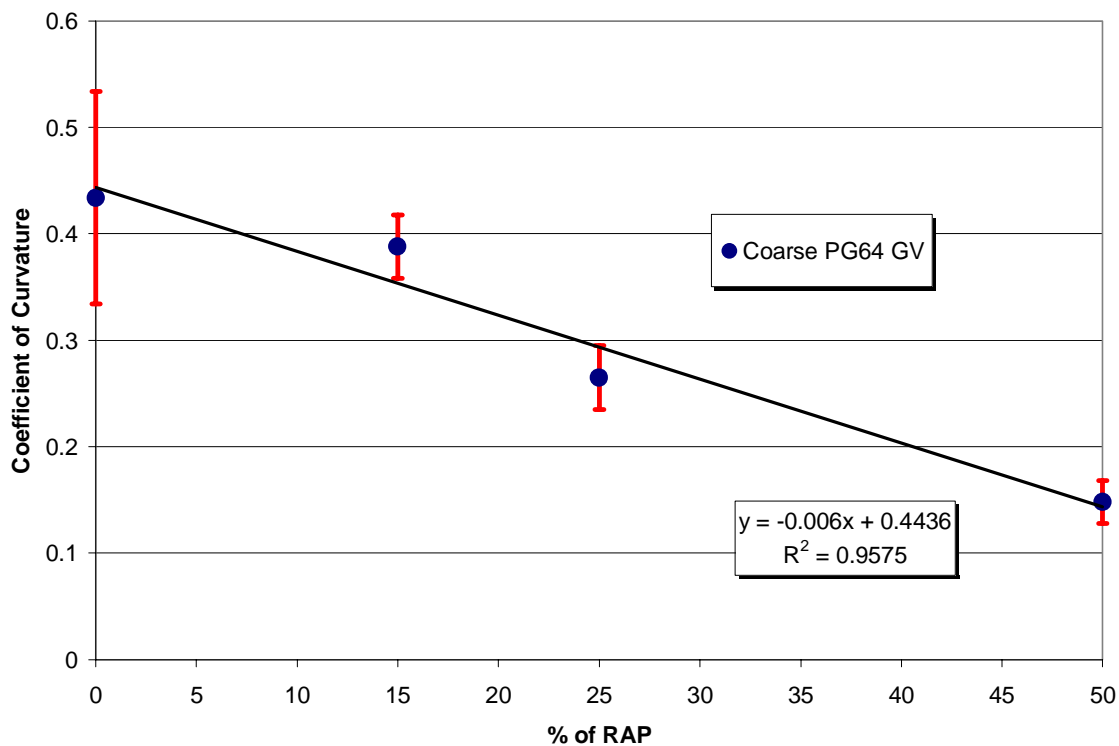
Figure 5.8: Relation between percent of RAP and
curvature coefficient (MN RAP, Gravel, PG 64-22, 22°C)

5.5 Practical Application of Findings

5.5.1 When to Change Virgin PG Binder Grade

Guidelines for when to reduce the PG grade of the virgin binder, shown in table 2.1, are based on the grade of the recovered RAP binders (McDaniel et al. 2001). The AL RAP

70
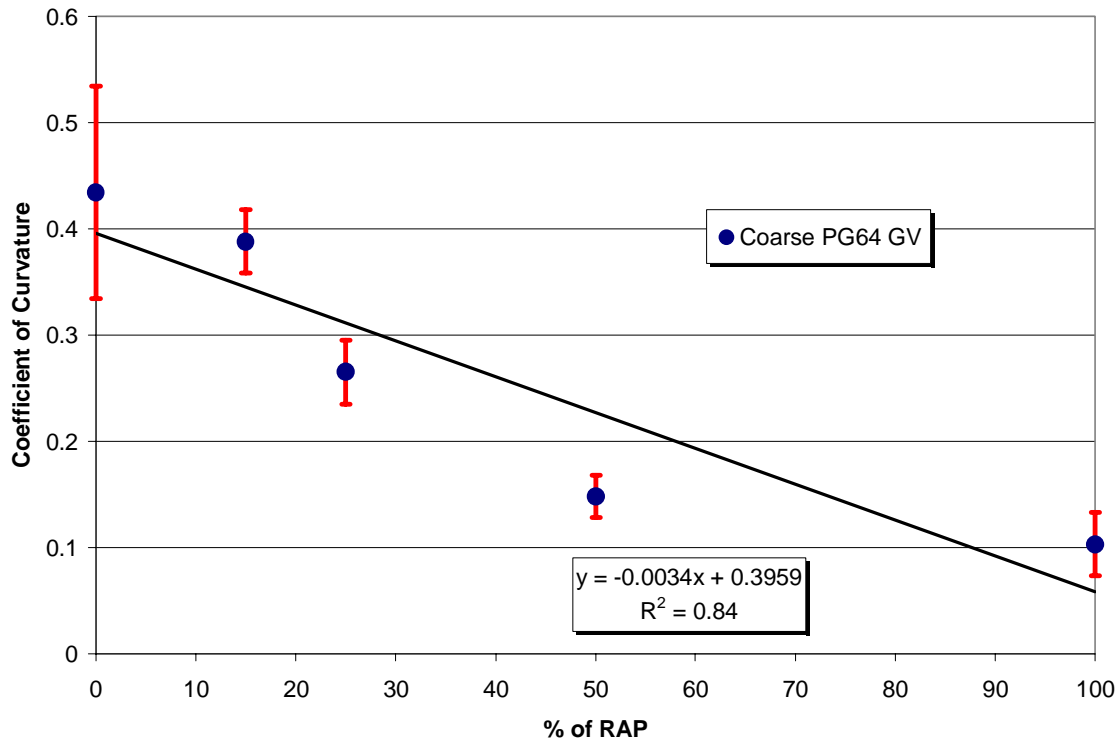
Figure 5.9: Relation between percent of RAP and
curvature coefficient (MN RAP, Gravel, PG 64-22, 22°C)

and MN RAP were graded as PG 88-16 and PG 88-10, respectively, so at the current ALDOT maximum of 15% RAP, mixes with either RAP source should have their PG binder grade reduced.

However, since ALDOT uses a midpoint PG grade (PG 67-22 instead of a PG 64-22) for specifying unmodified asphalt binders, this would mean that the PG grade would have to be reduced to a PG 58-28 to keep with the standard PG grading system. This may be too much of a reduction in the upper temperature stiffness, and could result in a substantial increase in rutting problems. RAP used in ALDOT mixes with a specified PG 76-22 would be increased to a PG 70-28.

An alternative approach can be developed based on the results of this study. Table 5.3 shows how the indirect tension stress relaxation parameters can be used to

71

replace the recovered binder NCHRP guideline recommendations. The data in tables in Tables 5.4a and 5.4b were used to estimate the percent change in the properties when 10% RAP, for the NCHRP guidelines, and 15% RAP, for the current ALDOT maximum allowable RAP. Estimated changes in properties assumed that changes are linear between 0 and 50% RAP.

Table 5.3 Alternative guidelines for when to consider changing PG grades

	NCHRP Guidelines		Current ALDOT Practice	
	Stress Relaxation Modulus (MPa)	Curvature Coefficient	Stress Relaxation Modulus (MPa)	Curvature Coefficient
Allowable change in mix properties before grade of virgin binder needs to be changed[1,2]	No more than 50% increase	No more than 12% decrease	No more than 75% increase	No more than 19% decrease

[1] % Changes expressed as changes in the mix properties compared with the same mix with no RAP
[2] Conditions for both the stress relaxation modulus and curvature coefficient need to be met

5.5.2 Determining the Percent RAP Actually Used in Construction

A practical application of this research is the determination of the percent RAP that can be used in a given HMA mixture. Using the concept that there is a linear relationship between the percent RAP from 0 to 50%, and both the initial stress relaxation modulus and the curvature coefficient, the percent RAP in a given mix can be determined as follows:

1. Mix and compact three samples for a control mix (no RAP) and three samples for a mix with the same aggregates and binder but with 50% RAP. The control gradation should be similar to that of the mix containing RAP. Use the same

virgin asphalt binder for both sets of samples.

2. Determine the initial stress relaxation modulus and curvature coefficient for the mix with no RAP and for the mix with 50% RAP.

3. Determine, b, the change in modulus for a percent change in RAP:

$$b = (M_{SR50} - M_{SR0}) / 50 \qquad\qquad \text{Eq. 5.3}$$

where:

M_{SR50} = initial stress relaxation modulus with 50% RAP

M_{SR0} = initial stress relaxation modulus with no RAP

4. Determine, $M_{SR?}$, the initial stress relaxation modulus for a mix with an unknown percent of RAP

5. Estimate the percent RAP in the mix:

$$\%RAP_M = (M_{SR?} - M_{SR0}) / b \qquad\qquad \text{Eq. 5.4}$$

where:

$\%RAP_M$ = estimated %RAP from initial relaxation modulus

The same process can be done with the curvature coefficient. Steps 1 and 2 would be the same, but then:

3. Determine, C, the change in curvature coefficient for a percent change in RAP:

$$C = (C_{50} - C_0) / 50 \qquad\qquad \text{Eq. 5.5}$$

where:

C_{50} = curvature coefficient with 50% RAP

C_0 = curvature coefficient with no RAP

4. Determine, $C_?$, the curvature coefficient for a mix with an unknown percent of RAP

5. Estimate the percent RAP in the mix:

$$\%RAP = (C_? - C_0) / C \qquad\qquad \text{Eq. 5.6}$$

where:

$\%RAP_C$ = estimated $\%RAP$ from curvature coefficient.

5.6 Test Method Refinements – Field Study

An evaluation of the initial test results showed that the standard deviation of both the initial stress relaxation modulus and curvature coefficient were dependent upon the mean value. The coefficient of variation (COV) was about 30% for the modulus and about 15% for the curvature coefficient. It was felt that the variability of both parameters could be reduced by conducting three tests per sample, then using the average of these three tests per sample as the single test result reported for each sample. Three tests can easily be obtained from the same sample by conducting one indirect tensile stress relaxation test, then removing the load, rotating the sample 30 degrees, testing again, then repeating the procedure for a third time. This way each test is conducted on a different area of the sample with each loading. Because the test method was originally set up so that the strains were within the LVE limits, then the assumption is that there is little or no significant damage to the sample. Since the time from start of loading the sample to the completion of one loading cycle takes less than 2 minutes, testing the same sample three times should only increase the testing time by about 3 to 4 minutes.

This change in the test method was combined with a preliminary evaluation of the consistency of binder properties during the production of a typical Alabama HMA (polymer modified asphalt binder) plant mixes which was obtained from East Alabama

Paving (EAP), a local paving company. One bag of HMA, taken by the plant staff during the day's production, was picked up each day for about 1 week by Auburn University researchers. This mix was reheated, split, and used to prepare five gyratory samples (100 gyrations). Samples for four days of HMA production were obtained, which means that a total of 20 samples were compacted and tested (see Appendix C). The same mix (coarse gradation, PG 76-22, no RAP) was produced on all four days of paving.

The indirect tension stress relaxation test was performed for this last portion of the research with the following test parameters:

- ram speed of 100 mm/min

- strain level around 0.0013

- test duration of 45 seconds
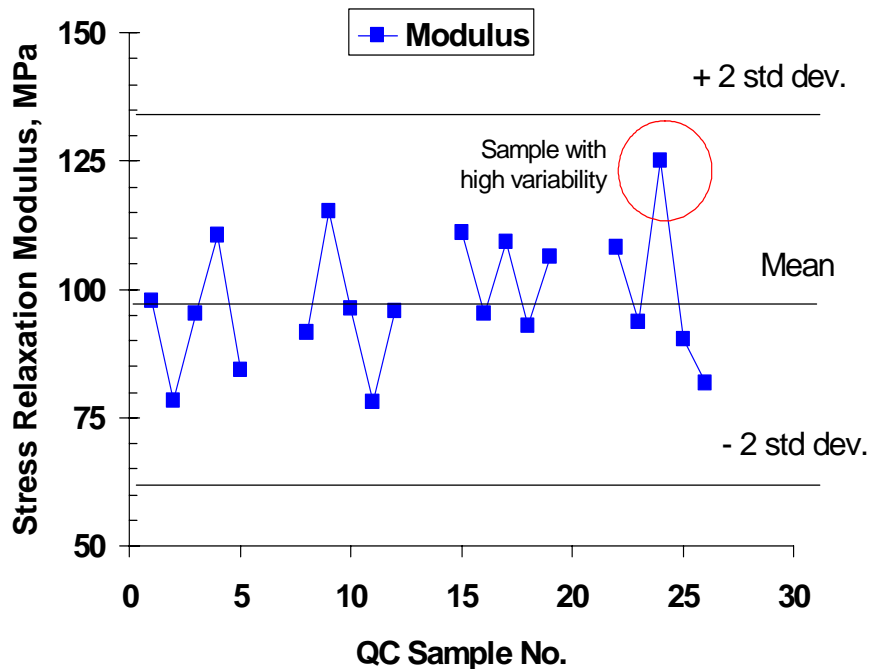
Figure 5.10: Modulus process control chart for field study

- data acquisition at every 0.1 second

- first three seconds of the test were not included in the analysis

The complete procedure, in ASTM format, can be seen in Appendix D.

Figure 5.10 shows the process control chart that is obtained for initial stress relaxation modulus for four days of paving as well as the plus and minus two standard deviation limits. The per bag variability, rather than per sample variability, is used to set the limits. All of the modulus values are well within the upper and lower limits.

Figure 5.11 shows the process control chart for the daily results for the curvature coefficient. While all of the values are within the limits, the curvature coefficient is more variable for the fourth day (samples 16 through 20), and once the outlier is removed, day 4 data shows a tendency to be higher than the other days.
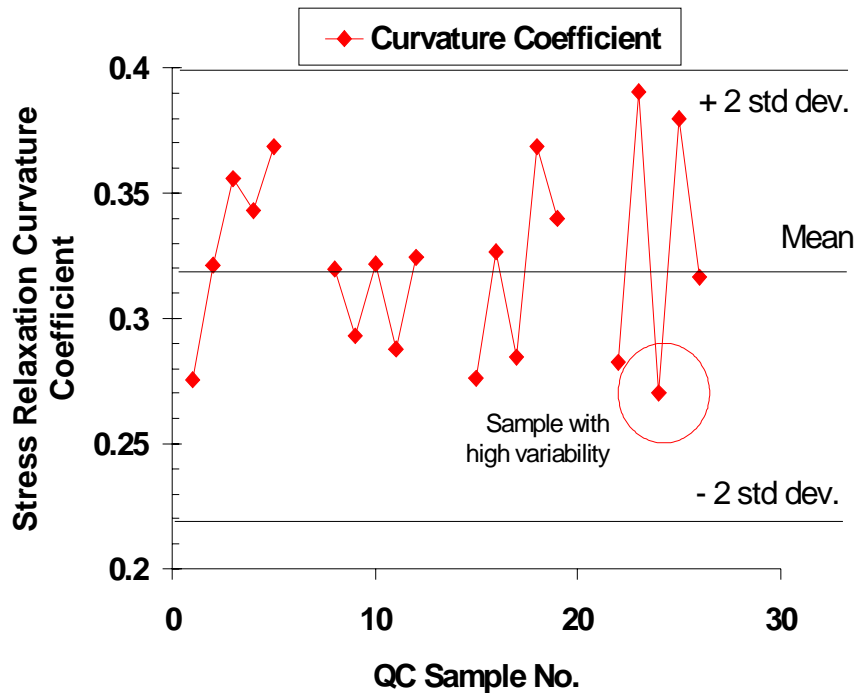
Figure 5.11: Curvature coefficient process control chart for field study

If the results from the EAP samples are compared with the results of the lab mixtures without RAP with the binder PG 76-22, it is found that the results are not statistically different for the modulus and for the curvature coefficient.

By doing three tests on each plant-produced sample without RAP, the COV was reduced from 30% to 18% for the initial stress relaxation modulus and to 7% (from 15% for the curvature coefficient.

5.7 Summary

When comparing the measured dynamic modulus and the calculated dynamic modulus from the stress relaxation test on the binder alone, it is obvious that the relation is really good, but not perfectly on the equality line. This is probably because two different DSR were used.

The relationship between the asphalt binder stress and the HMA mixtures stress relaxation moduli shows that the inclusion of any aggregate increases the initial stress relaxation by 1.5 to 2 orders of magnitude. There was little statistical difference in the initial stress relaxation modulus when one gradation was compared to another. These results indicate that while there is a large difference in the magnitude of the modulus when comparing binder-only to HMA samples, comparisons of one HMA mix result with another is not strongly dependent upon the gradation. Therefore, any changes in the modulus should represent a change in the effective HMA binder properties.

The use of a best fit power law curve is a good way to differentiate the stress relaxation results from different mixes. Two parameters are obtained from this curve fit: the initial stress relaxation modulus, and the curvature coefficient (exponent). The results

show that gradation, aggregate type and RAP source did not significantly influence either the stress relaxation modulus or the curvature coefficient. The grade of the binder had a small influence; reflecting the limited difference between the properties of the recovered RAP binders used in this study. The percent of RAP included in the mix had the largest effect on either parameter. The stress relaxation modulus increased with the addition of RAP up to 50%; there was no statistical difference in the modulus between mix containing 50 or 100% RAP. There was only a linear relationship between the percent of RAP and either parameter between 0 and 50% RAP. If 100% RAP is included, the relationship was non-linear for both the initial stress relaxation modulus and curvature coefficient.

CHAPTER 6 CONCLUSIONS AND RECOMMENDATIONS

6.1 Summary

The main objectives of this research were to develop and validate an indirect tension stress relaxation test using compacted HMA samples to evaluate binder properties and to evaluate the effect of adding RAP to an HMA mixture. Tests were performed in order to compare the stress relaxation results on binder alone with stress relaxation results on HMA. Then, mixes containing 0, 15, 25, 50 or 100% RAP were compacted with a Superpave gyratory compactor and tested in indirect tension stress relaxation at 5 and 22°C. The stress relaxation characteristics used in the analysis were the initial modulus and the curvature coefficient. The results were verified and the test method was refined in a field testing program.

6.2 Conclusion

The following conclusions are based on the observations and analysis presented in this paper:

1. Indirect tension stress relaxation test is a good indicator of the binder properties of the mix.

2. The gradation, aggregate source and RAP source have minimal influence on the stress relaxation characteristics in an indirect relaxation test for the range of mix variables used in this study.

3. There is a good correlation between the percentage of RAP in a mix and increases in the modulus of the mix. This relationship is linear only between 0 and 50% of RAP. This research suggests that the currently used assumption of a linear relationship between a change in binder stiffness and the percent of RAP (i.e., blending charts) is not a valid assumption. The relationship between modulus and the percent of RAP is non-linear, with the relationship between 50 and 100% being about asymptotic.

4. There is no significant difference in the modulus and the curvature coefficient for mix containing 50 or 100 percent RAP.

5. There is a good correlation between the percentage of RAP in a mix and the decrease of the curvature coefficient when between 0 and 50% RAP is used. This means that as the percentage of RAP increases, the ability of the mix to dissipate stress through deformation decreases.

6. Testing at an intermediate temperature, such as 22°C can be used as a single test temperature in order to evaluate the effect of RAP on HMA mixes.

7. The use of three tests per sample can decrease the coefficient of variation of the results.

8. The test is quick (5 minutes), simple to conduct, requires basic equipment (i.e. load cell, computer acquisition of data and time log, small load frame, and jack). With minor modifications, old Marshall stability load frames (with electronic load cells and RS232 port) can be used. Temperature control can be accomplished by placing sample in zip-lock bag, and bringing it to test temperature in a bulk specific gravity water tank.

9. Indirect tension stress relaxation testing has the possibility of being used as a process control test for contractors to monitor the consistency of the mix being produced.

6.3 Recommendations

These results suggest the following guidelines for the use of RAP:

- As little as 15% RAP will increase the mix modulus and decrease its ability to relax over time at cooler temperatures. RAP mixes should be used in the lower lifts of HMA pavements where an increase in stiffness could be beneficial and where daily thermal changes will be minimized.

- Using 15% and 25% RAP results in mixes with similar modulus and curvature coefficient at either test temperature. Therefore, it is preferable to use the higher percentage of RAP in lower lifts.

- Use of RAP in the wearing course is not recommended as this is the lift that will experience the highest temperature gradient. The highest curvature coefficient value is needed in this location in order to provide the most resistance to thermal and/or block cracking.

REFERENCES

1. Aklonis J.J., MacKnight W.J., **Introduction to Polymer Viscoelasticity**, Wiley-Interscience Publication, Second edition, 1983

2. Anderson D.A., Christensen D.W., Bahia H.U., Dongre R., Sharma M.G., Antle C.E., and Button, J., **Binder Characterization and Evaluation, Volume 3: Physical Characterization**, Strategic Highway Research Program, National Research Council, Report No. SHRP-A-369, 1994

3. APA, **Asphalt Pavement – The Recycling Leader Fact Sheet**, Asphalt Pavement Alliance, June 17, 2004, <http://www.asphaltalliance.com/upload/focus_recycling-FS.pdf>

4. ARRA, **Basic Asphalt Recycling Manual**, Asphalt Recycling and Reclaiming Association, Publication NHI01-022, 2001

5. Aphalt Institute, **Superpave Performance Graded Asphalt Binder Specification and Testing**, The Asphalt Institute Superpave Series No. 1 (SP-1), 1996

6. Azari H., McCuen R.H., and Stuart K.D., **Optimum Compaction Temperature for Modified Binders**, Journal of Transportation Engineering, ASCE, Vol 129, Sept/Oct 2003

7. Banasiak D., **States Plane Off Excess in RAP Specs**., Roads and Bridges, Vol. 34, No. 10, October 1996

8. Barnes H.A., **A Handbook of Elementary Rheology**, Institute of Non-Newtonian Fluid Mechanics, 2000

9. Baumgaertel M., and Winter H.H., **Determination of discrete relaxation and retardation time spectra from dynamic mechanical data**, Rheological Acta, Vol. #28, 1989

10. Bell C.A., **Aging of Asphalt-Aggregate Systems**, Summary Report, Strategic Highway Research Program Publications, SHRP-A-305

11. Behrens M.L., Dvorak B.I., and Woldt W.E., **Comparison of Asphalt Extraction Procedures, Implications of Hidden Environmental and Liability Costs**, Transportation Research Record, Vol #1661, 1999

12. Burr B.L., Davison R.R., Jemison H.B., Glover C.J., and Bullin J.A., **Asphalt Hardening in Extraction Solvents**, Transportation Research Record, Vol #1323, 1991

13. Buttlar W.G., Bozkurt D., Al-Khateeb G.G. and Waldhoff A.S., **Understanding Asphalt Mastic Behavior Through Micromechanics**, Transportation Research Record, Vol No. 1681, 1999

14. Carter A., **Rheologie en petite deformation des enrobes bitumineux et mesure de leur resistance a basse temperature a partir de l'essai TSRSTS**, Master Thesis, Ecole de technologie superieure, Montreal (Quebec), 2002

15. Chen T., **Determining a Prony Series for a Viscoelastic Material From Time Varying Strain Data**, NASA / TM-2000-210123, ARL-TR-2206, 2000

16. Cipione C.A., Davison R.R., Burr B.L., Glover B.L., and Bullin, J.A., **Evaluation of Solvents for Extraction of Residual Asphalt from Aggregates**, Transportation Research Record, Vol #1323, 1991

17. Cody R.P., and Smith J.K., **Applied Statistics and the SAS Programming Language**, Fourth Edition, 1997

18. Collin-Garcia H., Tia M., Roque R., and Choubane B., **Alternative Solvent for Reducing Health and Environment Hazards in Extracting Asphalt**, Transportation Research Record, Vol. #1712, 2000

19. Cosentino P.J., Kalajian E.H., Shieh C.S., Mathurin W.J.K., Gomez F.A., Cleary E.D., and Treeatrakoon A., **Developing Specifications for Using Recycled Asphalt Pavement as Base, Subbase or General Fill Materials: Phase II**, Florida Institute of Technology, Report No. FL/DOT/RMC/06650-7754, 2003

20. Cook R.D., and Young W.C., **Advanced Mechanics of Materials**, Second Edition, 1999

21. Curtis C.W., Ensley K., and Epps J., **Fundamental Properties of Asphalt-Aggregate Interactions Including Adhesion and Absorption**, Strategic Highway Research Program, SHRP-A-341, 1993

22. Daniel J.S. and Lachance A., **Rheological Properties of Asphalt Mixtures Containing Recycled Asphalt Pavement (RAP)**, Transportation Research Board Annual Meeting Proceeding, **TRB Paper No**.: 04-4507, 2004

23. Eighmy T.T., and Magee B.J., **The Road to Reuse**, Civil Engineering, The Magazine of the American Society for Civil Engineers, Vol. 71, No. 9, September 2001

24. Emery J.J., **Asphalt Concrete Recycling in Canada**, Transportation Research Record, Vol #1427, 1993

25. Fialka J., **EPA Asks Expert To Weigh Danger Of Solvent TCE**, Wall Street Journal, February 23, Vol 243, Issue 36, P. A8, 2004

26. Findley W.N., Lai J.S., and Onara K., **Creep and Relaxation of Nonlinear Viscoelastic Materials, With an Introduction to Linear Viscoelasticity**, Dover Publications, 1989

27. Garg N., and Thompson M.R., **Lincoln Avenue Reclaimed Asphalt Pavement Base Project**, Transportation Research Record, Vol #1547, 1996

28. Haddad Y.M., **Viscoelasticity of Engineering Materials**, Chapman & Hall, 1995

29. Hossain M., Metcalf D.G., and Scofield L.A., **Performance of Recycled Asphalt Concrete Overlays in Southwestern Arizona**, Transportation Research Record, Vol #1427, 1993

30. Huang B., Kingery W. R., Zhang Z. and Zuo G., **Laboratory Study of Fatigue Characteristics of HMA Surface Mixtures Containing RAP**, Transportation Research Board Annual Meeting Proceeding, TRB Paper No.: 04-4088, 2004

31. ISAP, **An Intensive Course on: Advanced Constitutive Modeling of Asphaltic Materials**, ISAP TC on Constitutive Modeling of Asphaltic Materials, University of Maryland-College Park, January 5-8 2005

32. Kandhal P.S., and Foo K.Y., **Designing Recycled Hot Mix Asphalt Mixtures Using Superpave Technology**, NCAT Report No. 96-5, 1997

33. Kandhal P.S., Rao S.S., Watson D.E., and Young B., **Performance of Recycled Hot-Mix Asphalt Mixtures in Georgia**, Transportation Research Record, Vol #1507, 1995

34. Kennedy T.W., Huber H.A., Harrigan E.T., Cominsky R.J., Hughes C.S., Von Quintus H., and Moulthrop J.S., **Superior Performing Asphalt Pavements (Superpave) : The Product of the SHRP Asphalt Research Program**, Strategic Highway Research Program, National Research Council, Report No. SHRP-A-410, 1994

35. Khanal P.P., and Mamlouk M.S., **Tensile Versus Compressive Moduli of Asphalt Concrete**, Transportation Research Record, Vol. #1492, 1995

36. Kim Y.R., Seo Y., King, M. and Momen M., **Dynamic Modulus Testing of Asphalt Concrete in Indirect Tension Mode**, Transportation Research Board Annual Meeting Proceeding, TRB Paper No.: 04-4992, 2004

37. Larsen D.A., **Demonstration and Evaluation of Superpave Technologies: Final Evaluation Report for CT Route 2**, Report No. FHWA-CT-RD 2219-F-02-7, 2003

38. Lytton R.L., J. Uzan, E.G. Fernando, R. Roque, D. Hiltunen, and S. Stoffels, **Development and Validation of Performance Prediction Models and Specifications for Asphalt Binders and Paving Mixes**, SHRP-A-357, 1993

39. Macosko C.W., **Rheology: Principles, Measurments and Application**, VCH, 1994

40. McDaniel R, Soleymani H., and Shah A., **Use of Reclaimed Asphalt Pavement (RAP) Under Superpave Specifications: A Regionnal Pooled Fund Project**, Report No. FHWA/IN/JTRP-2002/6, Purdue University, 2002

41. McDaniel R., and Anderson R.M., **Recommended Use of Reclaimed Asphalt Pavement in the Superpave Mix Design Method: Technician's Manual**, NCHRP Report #452, 2001

42. McDaniel R.S., Soleymani H., Anderson R.M., Turner P., and Peterson, R., **Recommended Use of Reclaimed Asphalt Pavement in the Superpave Mix Design Method**, NCHRP Web Document 30 (project D9-12): Contractor's Final Report, 2000

43. McGraw J., Iverson D., Schmidt G., and Olson J., **Selection of an Alternative Asphalt Extraction Solvent**, Minnesota Department of Transportation, Report # MN/RC-2003-35, 2001

44. Menard K.P., **Dynamic Mechanical Analysis, A Practical Introduction**, CRC, 1999

45. Nielsen L.E., and Landel R.F., **Mechanical Properties of Polymers and Composites**, Second edition, revised and expanded, Dekker, 1994

46. Paul H.R., **Evaluation of Recycled Projects for Performance**, Association of Asphalt Paving Technology, Vol. 65, 1996

47. Peterson J.C., **Chemical Composition of Asphalt Related to Asphalt Durability: State of the Art**, Transportation Research Record, Vol #999, 1984

48. Peterson J.C., Plancher H., Ensley E.K., Venable R.L., and Miyake, G., **Chemistry of Asphalt-Aggregate Interaction: Relationship with Pavement**

Moisture-Damage Prediction Test, Transportation Research Record, Vol #843, 1982

49. Riande E., Diaz-Calleja R., Prolongo M.G., Masegosa R.M., and Salom C., **Polymer Viscoelasticity, Stress and Strain in Practice**, 2000

50. Roberts F.L., Kandhal P.S., Brown E.R., and Kennedy T.W., **Hot Mix Asphalt Materials, Mixture Design, and Construction,** NAPA, Second Edition, 1996

51. Roque R., and Buttlar W.G., **The Development of a Measurement and Analysis System to Accurately Determine Asphalt Concrete Properties Using the Indirect Tensile Mode**, Association of Asphalt Paving Technology, Vol. 61, 1992

52. Rosen S.L., **Fundamental Principles of Polymeric Materials**, Second Edition, Wiley Interscience, 1993

53. Rowe G.M., and Pellinen T.K., **Consideration of Elastic and Viscous Components of Rheology Relating to the Permanent Deformation of Hot Mix Asphalt Pavements**, Recent Advances in Materials Characterization and Modeling of Pavement Systems, Geotechnical Special Publication No. 123, ASCE, 2003

54. Sargious M., and Mushule N., **Behavior of Recycled Asphalt Pavements at Low Temperature**, Canadian Journal of Civil Engineering, Vol. 18, 1991

55. Shenoy, A., **Determination of the Temperature for Mixing Aggregates with Polymer-Modified Asphalt**, International Journal of Pavement Engineering, Vol 2, No 1, 2001

56. Shoenberger J.E., Rollings R.S., and Graham R.T., **Properties of Microwave Recycled Asphalt Cement Binders**, Physiscal Properties of Asphalt Cement Binder, ASTM, STP 1241, 1995

57. Sondag M.S., Chadbourn B.A., and Drescher A., **Investigation of Recycled Asphalt Pavement (RAP) Mixtures**, Minnesota Departement of Transportation, Report No. MN/RC-220-15, 2002

58. Stroup-Gardiner M., and Nelson J.W., **Use of Normal Propyl Bromide Solvents for Extraction and Recovery of Asphalts Cements**, National Center for Asphalt Technologies, Report # NCAT 2000-06, 2000

59. Stuart K.D., **Methodology for Determining Compaction Temperature for Modified Asphalt Binders**, Federal Highway Administration, Report No. FHWA-RD-02-016, 2002

60. Taha R., Ali G., Basma A., and Al-Turk O., Evaluation of Reclaimed Asphalt Pavement Aggregates in Road Bases and Subbases, Transportation Research Record, Vol #1652, 1999

61. TA Instruments, **AR 2000 Rheometer**, Publication #PN 500106.002 Rev. D, 2003

62. Tam K.K., Joseph P., and Lynch D.F., **Five-Year Experience of Low-Temperature Performance of Recycled Hot Mix**, Transportation Research Record, Vol #1362, 1992

63. Tayebali A.A., Deacon J.A., and Monismith C.L., **Comparison of Axial and Diametral Resilient Stiffness of Asphalt-Aggregate Mixes**, Transportation Research Record, Vol. #1492, 1995

64. TFHRC, **Reclaimed Asphalt Pavement**, Turner-Fairbank Highway Research Center, August 2004, http://www.tfhrc.gov/hnr20/recycle/waste/rap132.htm

65. Tsai B.W., Kannekanti V.N., and Harvey J.T., **The Application of Genetic Algorithm in Asphalt Pavement Design**, Transportation Research Board Annual Meeting Proceeding, TRB Paper No.: 04-4941, 2004

66. Wallace K., and C.L. Monismith, **Diametral Modulus Testing on Nonlinear Pavement Materials**, Association of Asphalt Paving Technology, Vol. 49, 1980

67. Williams L.M., Landel R.F., and Ferry J.D., **The Temperature Dependence of Relaxation Mechanisms in Amorphous Polymers and Other Glass-Forming Liquids**, Journal of the American Chemical Society, Vol. 77, 1955

68. Wineman A.S., and Rajagopal K.R., **Mechanical Response of Polymer, An Introduction**, Cambridge University Press, 2000

69. Yildirim Y., Solaimanian M., and Kennedy T.W., **Mixing and Compaction Temperature for Superpave Mixes**, Association for Asphalt Paving Technologist, Vol. 69, 2000

70. Young R.J., and Lovell P.A., **Introduction to Polymer**, Chapman & Hall, Second Edition, 1994

APPENDIX A

Maximum RAP allowed in Pavement for each state

Use of RAP in all states as of 1996

State	Max RAP for Batch Plants (%)			Max RAP for Drum Plants (%)		
	Base	Binder	Surface	Base	Binder	Surface
Alabama	40	40	15	50	50	15
Alaska	-	-	-	-	-	-
Arizona	30	30	30	30	30	30
Arkansas	70	70	70	70	70	70
California	50	50	50	50	50	50
Colorado	15	15	15	15	15	15
Connecticut	40	40	40	40	40	40
Delaware	35	35	25	50	50	30
Florida	60	50	None	60	50	None
Georgia	25	25	25	40	40	40
Hawaii	30	None	None	40	None	None
Idaho	Open	Open	Open	Open	Open	Open
Illinois	50	25	15	50	25	15
Indiana	50	50	20	50	50	20
Iowa	Open	Open	Open	Open	Open	Open
Kansas	50	50	50	50	50	50
Kentucky	30	30	30	30	30	30
Louisiana	30	30	None	30	30	None
Maine	40	40	None	40	40	None
Maryland	Open	Open	Limit	Open	Open	Limit
Massachusetts	20	20	10	40	40	10
Michigan	50	50	50	50	50	50
Minnesota	59	50	30	50	50	30
Mississippi	30	30	15	30	30	15
Missouri	50	50	50	50	50	50
Montana	50	50	10	50	50	10
Nebraska	Not used	Not used	Not used	Open	Open	Open
Nevada	50	50	15	50	50	15
New Hampshire	35	35	15	50	50	15
New Jersey	25	25	10	25	25	10
New Mexico	Open	Open	Open	Open	Open	Open
New-York	50	50	None	70	70	None
North Carolina	60	60	60	60	60	60
North Dakota	50	50	50	50	50	50
Ohio	50	35	20	50	35	20
Oklahoma	25	25	None	25	25	None
Oregon	30	20	20	30	20	20
Pennsylvania	Open	Open	Open	Open	Open	Open
Rhode Island	30	30	None	30	30	None
South Carolina	30	25	20	30	25	20
South Dakota	Not used	Not used	Not used	50	50	50
Tennessee	15	Open	None	Open	Open	None
Texas	15	Open	Open	Open	Open	Open
Utah	Not used	Not used	Not used	25	25	25
Vermont	Specs	Specs	Specs	Specs	Specs	Specs
Virginia	25	25	25	25	25	25
Washington	Open	Open	Open	Open	Open	Open
West Virginia	Open	Open	Open	Open	Open	Open
Wisconsin	Open	35	20	Open	35	20
Wyoming	50	50	50	50	50	50

APPENDIX B

Tables of results for the HMA indirect stress relaxation test

RELAXATION CHARACTERISTICS (MODULUS / CURVATURE COEFFICIENT) FOR HMA MIXES AT 5°C

Temp. °C	Asphalt	Source of RAP	% of RAP	Granite				Gravel			
				Fine Grad.		Coarse Grad.		Fine Grad.		Coarse Grad.	
				Modulus (MPa)	Curvature coefficient	Modulus (MPa)	Curvature coefficient	Modulus (MPa)	Curvature coefficient	Modulus (MPa)	Curvature coefficient
5	PG 64-22	None	None	255	0.135	211	0.111	235	0.117	237	0.144
		AL RAP	15%	525	0.078	528	0.071	554	0.102	632	0.099
			25%	564	0.068	487	0.087	527	0.094	604	0.066
			50%	468	0.084	606	0.067	428	0.081	614	0.062
			100%	595	0.036	575	0.036	595	0.036	575	0.036
		MN RAP	15%	516	0.126	521	0.100	557	0.108	499	0.138
			25%	486	0.080	401	0.096	523	0.064	494	0.077
			50%	475	0.042	375	0.060	521	0.047	504	0.036
			100%	625	0.018	625	0.018	625	0.018	625	0.018
	PG 76-22	None	None	224	0.116	227	0.131	211	0.099	210	0.117
		AL RAP	15%	413	0.071	494	0.096	635	0.054	617	0.094
			25%	669	0.081	479	0.105	498	0.059	519	0.055
			50%	574	0.063	629	0.064	565	0.055	701	0.036
			100%	595	0.036	575	0.036	595	0.036	575	0.036
		MN RAP	15%	357	0.135	349	0.138	421	0.071	507	0.073
			25%	444	0.103	602	0.096	472	0.078	441	0.102
			50%	363	0.027	316	0.034	632	0.026	504	0.036
			100%	625	0.018	625	0.018	625	0.018	625	0.018

RELAXATION CHARACTERISTICS (MODULUS / CURVATURE COEFFICIENT) FOR HMA MIXES AT 22°C

Temp. ^{o}C	Asphalt	Source of RAP	% of RAP	Granite				Gravel			
				Fine Grad.		Coarse Grad.		Fine Grad.		Coarse Grad.	
				Modulus (MPa)	Curvature coefficient	Modulus (MPa)	Curvature coefficient	Modulus (MPa)	Curvature coefficient	Modulus (MPa)	Curvature coefficient
22	PG 64-22	None	None	101	0.349	86	0.376	120	0.334	131	0.434
		AL RAP	15%	322	0.268	189	0.267	139	0.318	166	0.401
			25%	304	0.244	246	0.256	191	0.318	152	0.301
			50%	231	0.253	245	0.226	203	0.255	163	0.318
			100%	217	0.209	274	0.201	217	0.209	274	0.201
		MN RAP	15%	211	0.360	181	0.289	219	0.325	203	0.388
			25%	210	0.210	175	0.249	307	0.255	276	0.265
			50%	257	0.068	305	0.165	236	0.184	303	0.148
			100%	267	0.103	267	0.013	267	0.103	267	0.103
	PG 76-22	None	None	94	0.220	79	0.268	120	0.207	103	0.290
		AL RAP	15%	150	0.200	180	0.226	221	0.212	169	0.258
			25%	173	0.199	140	0.225	233	0.210	208	0.235
			50%	270	0.118	165	0.186	253	0.136	169	0.109
			100%	217	0.209	274	0.201	217	0.209	274	0.201
		MN RAP	15%	127	0.273	116	0.233	260	0.020	187	0.257
			25%	194	0.266	100	0.231	191	0.188	176	0.219
			50%	280	0.091	266	0.091	237	0.050	192	0.067
			100%	267	0.103	267	0.103	267	0.103	267	0.103

92

APPENDIX C

Table of results for the field tests

RESULTS FROM FIELD TESTING

	Modulus (MPa)						Curvature					
bag	1	2	3	average	std deviation	COV	1	2	3	average	std deviation	COV
1	112.0	86.3	95.2	97.8	13.1	13.4%	0.278	0.267	0.281	0.275	0.007	2.7%
1	103.9	79.8	50.9	78.2	26.5	33.9%	0.341	0.352	0.271	0.321	0.044	13.7%
1	87.1	112.7	85.8	95.2	15.1	15.9%	0.376	0.352	0.339	0.356	0.019	5.3%
1	146.5	74.0	110.8	110.4	36.3	32.9%	0.316	0.346	0.368	0.343	0.026	7.6%
1	100.4	87.3	65.4	84.4	17.7	20.9%	0.359	0.356	0.391	0.369	0.019	5.3%
2	106.5	93.2	74.8	91.5	15.9	17.4%	0.346	0.307	0.306	0.320	0.023	7.1%
2	120.3	109.6	115.9	115.3	5.4	4.7%	0.270	0.304	0.305	0.293	0.020	6.8%
2	96.7	103.4	88.2	96.1	7.6	7.9%	0.346	0.315	0.305	0.322	0.021	6.6%
2	97.1	51.4	85.7	78.1	23.8	30.5%	0.271	0.330	0.262	0.288	0.037	12.8%
2	117.9	97.4	71.6	95.6	23.2	24.2%	0.348	0.299	0.327	0.325	0.025	7.6%
3	103.1	125.0	104.6	110.9	12.2	11.0%	0.291	0.271	0.266	0.276	0.013	4.8%
3	122.2	90.9	72.9	95.3	24.9	26.2%	0.339	0.281	0.360	0.327	0.041	12.5%
3	94.9	118.9	113.9	109.2	12.7	11.6%	0.310	0.273	0.270	0.284	0.022	7.8%
3	86.0	93.6	99.1	92.9	6.6	7.1%	0.381	0.345	0.380	0.369	0.021	5.6%
3	120.5	92.7	106.1	106.4	13.9	13.0%	0.332	0.318	0.369	0.340	0.026	7.8%
4	122.2	114.6	87.6	108.1	18.2	16.8%	0.294	0.269	0.285	0.283	0.013	4.5%
4	88.8	80.3	111.6	93.5	16.2	17.3%	0.360	0.402	0.410	0.391	0.027	6.9%
4	182.8	92.6	99.6	125.0	50.2	40.1%	0.293	0.248	0.269	0.270	0.023	8.3%
4	94.2	93.3	83.4	90.3	6.0	6.6%	0.382	0.371	0.387	0.380	0.008	2.2%
4	68.1	103.4	73.9	81.8	18.9	23.1%	0.250	0.357	0.342	0.316	0.058	18.3%

APPENDIX D

Draft standard for Indirect Tension Stress Relaxation Test on HMA to Evaluate the effect of the addition of RAP on the Binder Related Properties in the ASTM format

Designation: X XXXX-XX

Standard Test Method for
Indirect Tension Stress Relaxation to for Compacted Bituminous Mixtures[1]

This standard is issued under the fixed designation D XXXX; the number immediately following the designation indicates the year of original adoption or, in the case of revision, the year of last revision. A number in parentheses indicates the year of last reapproval. A superscript epsilon (ε) indicates an editorial change since the last revision or reapproval.

1. Scope

1.1 This test method covers the determination of the asphalt binder related properties of compacted HMA specimens by means of indirect tension stress relaxation. This test method can be used to evaluate the effect of the addition of RAP to a HMA mix.

1.2 The values stated in SI units are to be regarded as the standard. The value given in parentheses are for information only

1.3 *This standard does not purport to address all of the safety concerns, if any, associated with its use. It is the responsibility of the user of this standard to establish appropriate safety and health practices and to determine the applicability of regulatory limitations prior to use.*

2. Referenced Documents

2.1 *ASTM D979* Standard Practice for Sampling Bituminous Paving Mixture

2.2 D6925 Standard Test Method for Preparation and Determination of the Relative Density of Hot Mix Asphalt (HMA) Specimens by Means of the Superpave Gyratory Compactor[2]

---

[1] This test method is under the jurisdiction of ASTM Committee and is the direct responsibility of Subcommittee . [2]*Annual Book of ASTM Standards, Vol 04.03*

Current edition approved XXX. XX, XXXX. Published XX XXXX.

2.3 ASTM D3203 Standard Test Method for the Percent Air Voids in Compacted Dense and Open-Graded Bituminous Paving Mixtures.

3. Terminology

3.1 *Definitions of Terms Specific to This Standard:*

3.1.1 *Curvature coefficient*, n – exponent of a power law curve equation fit through indirect tension stress relaxation modulus over at least a 45 second time period from the start of the load application. The curvature coefficient represents the ability of the bituminous mixture to dissipate stress through deformation.

Initial stress relaxation modulus, n – the intercept for a power law curve fit through indirect tension stress relaxation modulus over at least a 45 second time period from the start of the load application. The stress relaxation modulus represents the maximum tensile stress the bituminous mixture exhibits immediately after the application of a given strain.

4. Significance and Use

4.1 The curvature coefficient and the initial stress relaxation modulus can be used to monitor changes in the bituminous mixture properties that are predominately related to the asphalt binder properties.

4.2 These values can be used to evaluate the influence of the percent of reclaimed asphalt pavement (RAP) on bituminous mixture properties. These values can also be used to evaluate the uniformity of RAP stockpiles.

5. Apparatus

5.1 *Caliper*– digital or manual caliper with a precision of 0.1 mm.

5.2 *Water Bath*- capable of maintaining by any means, a constant temperature between 20 and 30°C (70 to 85°F). The water bath must be suitable for immersion of the sample to be tested.

5.3 *Diametral testing jig* - as shown in Figure 1.

5.4 *Load cell*

5.5 Load frame - a load frame with an adjustable platform. The movement of the platform shall be sufficient to allow the application of a maximum of a 10 lb seating load on the sample after it has been loaded in the diametral testing jig.

Note 1: A Marshall stability load frame is an example of an acceptable load frame.

6. Sampling

6.1.1 Obtain field samples in accordance with Practice D 979.

6.2 Alternatively, obtain 150 mm (6 inch) diameter cores from bituminous pavements. Care shall be taken to avoid distortion, bending, or cracking of the specimens during and after removal from pavements. Specimens shall be stored in a safe, cool place. Specimens shall be free of foreign materials such as seal coat, tack coat, foundation material, soil, paper, or foil.

7. Sample Preparation

7.1 Compact three specimens according to ASTM D6925 using either laboratory prepared or field sampled bituminous mixtures.

7.2 All samples shall be compacted so that the air voids target 4% air voids +/- 1% according to ASTM D3203.

7.3 If cores are used, specimens shall be separated from other pavement layers by sawing or other satisfactory means. Each specimen shall represent, as closely as possible, a single layer of homogeneous bituminous mixture with no height less than 25 mm (1 inch).

8. Procedure

8.1 Use a marker such as a construction crayon or paint pen to mark points around the circumference of the specimen at 0, 30, and 60°. Mark three additional points at 180° from each of these positions.

8.2 Place the specimens in a waterproof bag, such as a zip-lock^{TM} bag, and submerged in the water bath at 25^oC for a minimum of 1 hour. Care should be taken so that the plastic does not allow water into the sealed bag,

8.3 After 1 hour, remove the specimen from the water, and then remove the specimen from the bag.

8.4 Immediately place the specimen on the lower platen of the diametral jig.

8.5 Align the top and bottom loading strips with the first point on the circumference of the specimen.

8.6 Move the loading frame platform up so that no more than 10 lb of seating load is applied to the specimen.

8.7 Quickly apply the step strain.

8.8 Maintain the firm contact for 45 seconds and record the changing stress during that period.

8.9 Release the strain and ensure that the specimen will not fall off the loading strips. If the specimen falls from the setup, take note of it because it might be damaged and the results can be misleading.

8.10 Rotate the specimen 30°, so it is aligned with the second diameter line, and start the test over. Redo the same thing on the third diameter line.

8.11 Determine the diameter of the test specimen by averaging three measurement of the diameter taken evenly spaced on the specimen.

8.12 Determine the height of the test specimen by averaging three measurement of the height taken evenly spaced on the specimen.

9. Calculation or Interpretation of Results

9.1 Calculate the tensile stress in the specimen with:

$$T = \frac{2P}{\pi l d}$$

Where:

T = tensile stress (kPa)

P = applied load by the testing machine (kN)

l = length of the specimen (m)

d = diameter of the specimen (m)

9.2 Calculate the horizontal strain with:

$$\varepsilon_h = \varepsilon_v \, \mu$$

Where:

ε_h = horizontal strain

ε_v = vertical strain

μ = Poisson's ratio (0.2 at 5°C and 0.35 at 22°C)

9.3 Calculate the stress relaxation modulus (E) for every time increment available with:

$$E = \frac{T}{\varepsilon_h}$$

9.4 Draw the stress relaxation modulus versus the time and calculate a best fit power curve starting at 3 seconds. If the load frame used can reach and keep a constant strain in a shorter time, than plot the best fit curve starting earlier.

9.5 Use the initial modulus and the curvature coefficient of the equation of the best fit power curve to do the analysis.

10. Report

10.1 Report the following information:

10.1.1 Proper identification of the samples,

10.1.2 Constant horizontal strain and the poisson's ratio used to calculate it,

10.1.3 Graphical representation of the relaxation modulus versus time,

10.1.4 Initial modulus, curvature coefficient and the r^2 correlation factor of the power curve,

10.1.5 Apparatus used to determine test values.

11. Precision and Bias

11.1 *precision* – The single operator and multilaboratory precision of tests of individual Superpave gyratory compacted HMA samples is given for samples made in a laboratory environment and under normal field conditions.

	Coefficient of Variation (percent of mean)[A]	Acceptable Range of Two Results (percent of mean)[A]
Single Operator Precision		
Relaxation Modulus (22°C)	0.18	0.50
Curvature Coefficient (22°C)	0.07	0.20
Multilaboratory Precision		
Relaxation Modulus (22°C)	0.21	0.59
Curvature Coefficient (22°C)	0.13	0.36

[A] These numbers represent, respectively, the (1s%) and the (d2s%) limits as described in Practice C 670

11.2 *Bias* – Since the relaxation modulus and curvature coefficient can be defined only in terms of a test method, no bias statement is being made.

12. Keywords

12.1 Reclaimed Asphalt Pavement, RAP, Bituminous Mixtures, Indirect Tension, Relaxation Modulus, Curvature Coefficient

Figure 1: Indirect Tension Setup